

REMARKS

Claims 1-24 and 27-29 are pending in the application. Claims 25 and 26 were previously cancelled. Claims 30 and 31 are added herein. Thus, claims 1-24 and 27-31 are now under consideration.

Claim 1 is amended for additional clarity. No new matter is added by this amendment. Support for this amendment is found throughout the as-filed specification and original claims.

Claims 2 and 4 are amended based on suggestions made by the Examiner. No new matter is added by these amendments. Support for these amendments is found throughout the as-filed specification and original claims.

New claims 30 and 31 include no new matter and are supported throughout the as-filed specification and original claims.

For example, in regard to selecting the sperm type, wherein the selected sperm type has a desired characteristic selected from a group consisting of low levels of DNA damage, the Applicants refer to Figure 3 for support. Figure 3 show results of TUNEL assays. TUNEL is a common method for detecting DNA fragmentation and damage. A TUNEL-positive cell has DNA damage. Thus, in Figure 3, a sperm population with a higher percentage of TUNEL-positive cells is a population containing a higher percentage of DNA damaged cells. The data displayed in Figure 3 show that all electrophoretically separated populations had a lower percentage TUNEL-positive sperm than the sperm population that did not traverse the membrane.

Moreover, when Figures 1-8 are reviewed in light of Figure 9 the data show that sperm are being separated into separated and excluded populations, including morphology (Figure 1), sperm deformity index (Figure 2), DNA damage (Figure 3), acrosome reaction (Figure 4), post treatment vitality (Figure 5), post treatment motility (Figure 6), computer assisted sperm analysis (Figures 7 and 8). The figures show that differences in desired outcome for the desired characteristics were observed for morphology, sperm deformity index, DNA damage, acrosome reaction, and computer-assisted sperm analysis. Figure 9 displays the yield. Although the zero time point does show differences in characteristics, the sperm numbers relate to only about 2% yield and these represent the most motile sperm that swam through the membrane. Useful yields

are obtained after application of the electrical potential, which are indicated at subsequent time points in the figure. Thus, taken together Figures 1-9 show separation of sperm types listed in new claims 30 and 31. In addition, claims 30 and 31 recite other sperm types acknowledged as enabled by the examiner. For these reasons, Applicants submit that the new claims are supported and enabled by the filed application.

I. Interview Summary.

The Applicants thank Examiner Noguerola for the in-person interview on June 03, 2011 in which the 35 U.S.C. § 112 and 35 U.S.C. § 103(a) rejections were discussed without reaching agreement.

II. 35 U.S.C. § 102(b) Su.

Claims 1-3, 6, 7, 12, 13, 17, 20 and 21 are rejected under 35 U.S.C. § 102(b) as allegedly anticipated by an English language translation of CN 89105110.5 ("Su"). Su, however, fails to disclose separation of a sperm type by moving sperm through an ion-permeable barrier where the sperm type is separated from a sperm population through the ion-permeable barrier.

The Examiner argues that Su's semi-permeable bag must be permeable to ions. The Applicants do not herein dispute this assessment.

The figures from Su, viewed with reference to pages 4-6 of the description, show that the electrodes (2 and 5) are located outside of the electrophoresis cell (4). These facts are recognized by the Examiner at page 15 of the Office Action. Because the electrophoresis cell is the semi-permeable bag, the electrodes are outside of the semi-permeable bag.

Therefore, when the sperm sample is placed inside the cell it is separated from the electrodes by the bag's walls. The bag is permeable to ions so that an electrophoresis field can be established inside the cell and through the sperm sample. Otherwise, as articulated by the Examiner, the electrolyte would be blocked and the electrophoresis field would be disrupted.

The Applicants follow the Examiner's arguments to this point. The Examiner, however, then concludes that sperm inherently moves through the semi-permeable bag. This conclusion

incorrect (a) because the sperm in Su do not necessarily move through an ion-permeable membrane and (b) because Su actually teaches away from moving sperm through an ion-permeable membrane.

a. The sperm in Su do not inherently move through an ion-permeable membrane.

To arrive at his conclusion that Su inherently teaches movement of sperm through an ion-permeable, the Examiner notes that Su teaches that semen is collected “at the anode.” Because semen is collected “at the anode,” the Examiner believes that sperm must have inherently moved through the semi-permeable bag (*i.e.* ion-permeable membrane). The term “at” does not, however, necessarily mean or imply direct contact of semen with the anode. Common definitions of the term “at” include “in or near the area occupied by” or “in or near the location of.” See definition 1.a. of “At” from the Free Online Dictionary, Thesaurus and Encyclopedia (Exhibit A). The semen found “at the anode” could, therefore, be near or in the area of the anode without having passed through the bag’s walls. For example, the semen could be contained in the electrophoresis cell in proximity to the anode, but still separated from the anode by the chamber walls.

The fact that a certain result or characteristic may occur or be present in the prior art is not sufficient to establish the inherency of that result or characteristic. *In re Rijckaert*, 9 F.3d 1531, 1534 (Fed. Cir. 1993); *In re Oelrich*, 666 F.2d 578, 581-82 (CCPA 1981) (emphasis added). “To establish inherency, the extrinsic evidence must make clear that the missing descriptive matter is necessarily present in the thing described in the reference, and that it would be so recognized by persons of ordinary skill. Inherency may not be established by probabilities or possibilities. The mere fact that a certain thing may result from a given set of circumstances is not sufficient.” *In re Robertson*, 169 F.3d 743, 745 (Fed. Cir. 1999) (emphasis added). Since inherent anticipation, therefore, requires an event to necessarily have happened, Su does not inherently anticipate the rejected claims because sperm does not necessarily move through an ion-permeable membrane using Su’s method or device.

The Examiner implies that, just because Su collected an enhanced population of X semen at the anode, the collected X semen must have moved through a membrane. This is not true. It was known to those skilled in the art before Su that X and Y semen have different zeta potentials, with the X being more negative, such that directing a current through the sample from cathode to anode could cause an enhanced population of X semen at an anode without passing through a membrane. *See e.g.* Ishijima SA et al., Zeta potential of human X- and Y-bearing sperm, International Journal Andrology 14(5): 340-7 1991 (Abstract) attached as Exhibit B. *See also*, Engelmann et al., Gamete Res. 19, 151-159 (1988) (Engelmann) cited by the Examiner in the current Office Action.

b. Su teaches away from moving sperm through an ion-permeable membrane.

Su describes that the semi-permeable bag is actually used to *prevent* direct contact between semen and the [anode]. For example, on page 5 Su states “the design of the electrophoresis cell used can prevent direct contact between the semen and the electrodes.”

Thus, based on the common definition of “at” and the explicit teaching of Su, the semen does not appear to contact the anode at all. In fact, Su intentionally avoids passing sperm through an ion-permeable membrane to avoid contact of semen with the electrodes.

For at least these reasons, Su does not inherently anticipate the rejected claims. Applicants request that the rejection of these claims based on Su be withdrawn.

III. 35 U.S.C. § 103(a) Moore in view of Speicher.

Claims 1, 5-10, 12, 13 and 17-19 are rejected under 35 U.S.C. § 103(a) as allegedly unpatentable over Moore et al., J Reprod. Fert. 44, 329-332 (1975) (Moore) and Speicher et al., U.S. Pat. No. 6,638,408 (Speicher). In regard to claim 1, the Examiner alleges that Moore discloses a process of separating a sperm type from a sperm population by electrophoresis using a pH-gradient. The Examiner acknowledges that Moore fails to disclose use of an ion-permeable barrier.

The Examiner further alleges that Speicher discloses a separation chamber portioned by ion-permeable membranes. The Examiner acknowledges that Speicher fails to disclose separation of sperm type from a sperm population.

The Examiner, however, alleges that it would have been obvious to one skilled in the art to use the isoelectric focusing device of Speicher to practice the method of Moore with predictable results.

The Applicants respectfully traverse these rejections because (a) the combined references are inoperable for their cited purpose and (b) the results of the Applicants' claimed processes provide surprising and unexpected results over the cited references.

(a) The 35 U.S.C. § 103(a) rejection is improper because the combination of Speicher and Moore is inoperative for its cited purpose.

The membranes described in Speicher have pores too small, less than 0.5 μm , to allow sperm to pass through. *See* Speicher, col. 5:55-65. At least because the pores of Speicher are too small to allow sperm to pass through, if Speicher were combined with Moore, the resulting device would not work to separate sperm. In other words, if the membranes described by Speicher were used with a sperm sample, none of the sperm would be able to pass through the membrane. Thus, a device combining Moore and Speicher would not work to separate a sperm type from a population by moving sperm through a membrane because sperm cannot move through the described membrane. Thus, the combination of Moore and Speicher is *inoperable* to separate a sperm type from a sperm population through an ion-permeable barrier.

“An inference that a combination would not have been obvious is *especially strong* where the prior art's teachings undermine the very reason being proffered as to why a person of ordinary skill would have combined the known elements.” *DePuy Spine Inc. v. Medtronic Sofamor Danek, Inc.* 567 F.3d 1314, 1326 (Fed Cir. 2009) (emphasis added). *See also* Examination Guidelines Update: Developments in the Obviousness Inquiry After KSR v. Teleflex, Fed. Reg. 53,643, 53,649 (Sept 1, 2010).

Here the reason proffered for the combination of Moore and Speicher is to separate sperm, which cannot be achieved with the combination because of the membrane characteristics of Speicher. Any method disclosed by Moore and Speicher in combination would not have worked for the intended purpose of separating sperm.

Although the Examiner indicates that Speicher teaches adjusting pore size, the Examiner does not allege that Speicher teaches, either inherently or otherwise, a pore size capable of allowing the passage of sperm. On page 18 of the Office Action, the Examiner states Speicher teaches adjusting the pore size so that the desired “particles” can pass through. The only desired “particles” Speicher describes, however, are “charged molecules.” One skilled in the art would not interpret the term “charged molecule” to include a sperm cell. The only mention in Speicher of cells are cell extracts, and Speicher describes lysing cells prior to any separation so that the inner cellular molecules are separated, not the cells themselves. See Speicher col. 7:40-col.8:25. Speicher, therefore, only separated charged molecules, not cells, and its suggestion to adjust pore size for “desired particles” would not lead one skilled in the art to pores sufficiently sized to separate sperm cells.

Moreover, the polyacrylamide membranes described by Speicher would not form stable membranes with pores large enough to separate sperm. For example, Chiari et al., *Electrophoresis* 1995 16(8) 1337-44 (enclosed as Exhibit D) describes that polyacrylamide will not form a stable matrix much below 3.5% unless supported by another material. *See e.g.* Chiari, figure 6 showing that data points for a pure polyacrylamide gel stop at about 4%. Since pore size in such a membrane would not be close to being larger enough to separate cells, the Speicher membranes would not function to separate cells given the tiny pore size. *See e.g.* Stellwagen and Holmes, *Electrophoresis* 1991 Apr 12(4) 253-63 (describing 3.5% gels having a pore size of 130nm and 10.5% gels having 70nm pores) (enclosed as Exhibit E). Therefore, the membranes of Speicher would not have been expandable to separate sperm cells.

(b) The claimed methods provide unexpected results.

Assuming, *arguendo*, that Speicher did disclose, or even suggest, pores of sufficient size to separate sperm, the current application still provides unexpected results over the Speicher and Moore combination. Moore discloses that the sperm cells separated using its method were “immotile.” *See* Moore, page 330, line 16. As noted in the Applicants’ response to the September 10, 2009 Office Action, the claimed processes produce sperm which are “substantially unchanged.” For example, sperm separated by the claimed processes maintain their fertilizing potential and other properties such as motility. These unexpected results are described in the Applicants’ previous amendment, but the Examiner does not appear to have considered them.

For these reasons, Applicants respectfully request the withdrawal of the rejection of claim 1. Since claims 5-10, 12, 13 and 17-19 all ultimately depend from claim 1 and include all the elements of claim 1, these claims are also non-obvious over the cited references, and the Applicants request withdrawal of the rejection of these claims as well.

IV. 35 U.S.C. § 103(a) Moore in view of Speicher in further view of Barbour.

Claim 11 is rejected under 35 U.S.C. § 103(a) as allegedly being unpatentable over Moore, as modified by Speicher, and in further view of Barbour et al., U.S. Patent No. 5,436,000 (Barbour). Claim 11 ultimately depends from claim 1. The Applicants, therefore, respectfully traverse this rejection for the same reasons described above regarding the rejection of claim 1 based on Moore as modified by Speicher.

Specifically, as described above, any method disclosed or suggested by Moore and Speicher in combination is inoperable for separating a sperm type. As noted above, 0.5 microns is the upper pore size limit described in Speicher, and this pore size is too small to allow sperm to pass. *See* Speicher, col. 5:55-65.

Moreover, the method of claim 11 provides unexpected results in view of Moore as modified by Speicher. Moore and Speicher describe immotile sperm and no separation of sperm, respectively, so their combination fails to disclose or suggest the results achieved using the process of claim 11. Barbour does not overcome the deficiency of the Moore and Speicher

combination in this regard. Barbour is cited as disclosing polycarbonate membrane as an ion-permeable barrier. The cited disclosure of Barbour is unrelated, however, with whether sperm separated through a membrane by a method resulting from the combination of Moore as modified by Speicher would be substantially unchanged. Thus, Barbour fails to disclose or suggest the results achieved with the process of claim 11, even when Barbour is read in combination with Moore and Speicher. The Applicants, therefore, respectfully request withdrawal of this rejection.

V. 35 U.S.C. § 103(a) Moore in view of Speicher in further view of Moore II.

Claims 2, 3 and 14 are rejected under 35 U.S.C. § 103(a) as allegedly being unpatentable over Moore, as modified by Speicher, and in further view of Moore, Int. J. Andro. 2: 449-452 (1979) (Moore II). Claims 2, 3 and 14 ultimately depend from claim 1. The Applicants, therefore, respectfully traverse this rejection for the same reasons described above regarding the rejection of claim 1 based on Moore as modified by Speicher.

Specifically, as described above, any method disclosed or suggested by Moore and Speicher in combination is inoperable for separating a sperm type. Moreover, the methods of claims 2, 3 and 14 each provide surprising and unexpected results in view of Moore as modified by Speicher. Moore and Speicher describe immotile sperm and no separation of sperm, respectively, so their combination fails to disclose or suggest the processes of claims 2, 3 and 14. Moore II fails to overcome the deficiency of the Moore and Speicher combination. Moore II is cited as teaching that spermatozoa from some “apparently infertile men have an isoelectric point consistently higher than fertile men.” The cited disclosure of Moore II is unrelated, however, with whether sperm separated through a membrane by a method resulting from the combination of Moore as modified by Speicher would be substantially unchanged. Thus, Moore II fails to disclose or suggest the results achieved with the processes of claims 2, 3, or 14, even when Moore II is read in combination with Moore and Speicher. The Applicants, therefore, respectfully request withdrawal of this rejection.

VI. 35 U.S.C. § 103(a) Moore in view of Speicher in further view of Jaspers, Raptis and Burke Jr.

Claims 14 and 15 are rejected under 35 U.S.C. § 103(a) as allegedly being unpatentable over Moore, as modified by Speicher, and in further view of Jaspers et al., App. Evn. Micro. 3176-3181 (1997) (Jaspers), Raptis, U.S. Pat. No. 6,001,617 (Raptis), and Burke Jr. et al., U.S. Pat. App. Pub. No. 2002/0119218 (Burke Jr.). Claims 14 and 15 ultimately depend from claim 1. The Applicants respectfully traverse these rejections for the same reasons described above regarding the rejection of claim 1 based on Moore as modified by Speicher.

Specifically, as described above, the combination of Moore and Speicher is inoperable for separating a sperm type. Moreover, claims 14 and 15 each provide surprising and unexpected results in view of Moore as modified by Speicher. Moore and Speicher describe immotile sperm and no separation of sperm, respectively, so their combination fails to disclose or suggest the results achieved using the processes of claims 14 and 15. Jaspers, Raptis and Burke Jr., are cited for their described voltage gradients. The cited disclosures of these references are unrelated, however, with whether sperm separated through a membrane by a method resulting from the combination of Moore as modified by Speicher would be substantially unchanged. Thus, Jaspers, Raptis and Burke Jr. fail to disclose or suggest the results achieved with the processes of claim 14 and 15, even when the cited references are read in combination with Moore and Speicher. The Applicants, therefore, respectfully request withdrawal of this rejection.

VII. 35 U.S.C. § 103(a) Engelmann in view of Weber.

Claims 1-10, 12-23, 28 and 29 are rejected under 35 U.S.C. § 103(a) as allegedly unpatentable over Engelmann et al., Gamete Res. 19, 151-159 (1988) (Engelmann), which was originally cited in the September 10, 2009 Office Action, in view of Weber, U.S. Patent No. 7,399,394 (Weber).

In making the current rejection based on Engelmann and Weber, the Examiner alleges that Engelmann teaches a method of sperm separation based on electrophoretic mobility and that Weber discloses a method for separating charged substances with an ion-permeable membrane.

However, nothing in Weber teaches or suggests separation of cells through a membrane. Thus, the combined references do not provide a *prima facie* case of obviousness at least because they do not together disclose separation of sperm through a membrane. Moreover, assuming, *arguendo*, the Engelmann and Weber combination does present a *prima facie* case of obviousness, the current application describes unexpected results over the cited combination.

Engelmann discloses or suggests that the motility of sperm separated by free flow electrophoresis is "greatly reduced." See Engelmann, page 156. For example, Engelmann shows motility in the range between 5% and 10% or 10% and 20%. One skilled in the art would expect even more damage to separated sperm if an ion-permeable membrane was used to separate the sperm. See Amendment and Response to Office Action of September 10, 2009, page 8 and Amendment in Reply to Office action of June 11, 2010, page 11. Thus, one skilled in the art would expect at least 80% of the sperm to have reduced motility using Engelmann with a membrane. On the other hand, the Examiner notes that the Applicants show 84% of the sperm were still motile.

The Examiner incorrectly states on page 6 of the Office Action that the Applicants did not measure a change in motility other than whether the sperm moved or not. For example, paragraph 117 of the application states that "separated spermatozoa displayed track speeds and levels of path and forward progressive velocities that were not significantly different than those recorded in the excluded population." Engelmann specifically states that progressive motility was *greatly* reduced. See Engelmann, page 156. Progressive motility relates to velocity. See *e.g.* Engelmann et al., J. Andrology 13(5) 433-436 (1992), enclosed as Exhibit C, which describes that progressive motility relates to sperm having a given velocity and that quantitative sperm motility relates to velocity. Thus, when Engelmann (1988) states that sperm motility was greatly reduced this would include changes in velocity. The fact that Applicants found no significant difference in progressive velocity and track speed is, therefore, surprising and unexpected in light of Engelmann and Weber.

Therefore, even if the Examiner maintains that a *prima facie* case has been properly established, the unexpected, superior results rebut a *prima facie* case of obviousness (See MPEP

§ 2144.09) and the Applicants respectfully request withdrawal of the rejection. The method *produces* unexpected superior results over Engelmann and Weber, which rebuts any *prima facie* case of obviousness.

Since claims 2-10, 12-23, 28 and 29 all ultimately depend from claim 1 and include all of the elements of claim 1, the Applicants respectfully request withdrawal of the rejection as to claim 1 and these dependent claims for the same reasons.

VIII. 35 U.S.C. § 103(a) Engelmann in view of Weber in further view of Barbour.

Because the Examiner withdrew the rejection of claim 11 based on Engelmann in view of Weber in further view of Barbour and did not restate the rejection, it appears that claim 11 is no longer rejected in light of this combination. However, on page 7 of the Office Action, the Examiner appears to believe the rejection still has merit. Therefore, to efficiently move this case to allowance, Applicants provide the following comments.

Claim 11 ultimately depends from claim 1. As explained above, the results of claim 1, and therefore, of claim 11, are surprising and unexpected in light of Engelmann as modified by Weber. Barbour is cited for its disclosure of polycarbonate membrane materials. The disclosure of Barbour does not make the results of claim 11 predictable in light of the Engelmann and Weber combination. The Applicants, therefore, respectfully request that the Examiner indicate allowability of claim 11 over this combination.

IX. 35 U.S.C. § 103(a) Su in view of Christensen.

Because the Examiner withdrew the rejection of claims 18 and 19 based on Su in view of Christensen and did not restate the rejection, it appears that claims 18 and 19 are no longer rejected in light of this combination. However, on page 7 of the Office Action, the Examiner appears to believe the rejection still has merit. Therefore, to efficiently move this case to allowance, Applicants provide the following comments.

As described above, Su does not teach or suggest that a sperm type moves through an ion-permeable barrier and is separated from a sperm population through the ion-permeable

barrier. Christensen is cited for a device to count bovine sperm. Thus, the combination of Su and Christensen fails to disclose or suggest that a sperm type moves through an ion-permeable barrier and is separated from a sperm population through the ion-permeable barrier, which is required by claims 18 and 19. The Applicants, therefore, respectfully request that the Examiner indicate allowability of claims 18 and 19 over this combination.

X. 35 U.S.C. § 103(a) Su in view of Kricka.

Because the Examiner withdrew the rejection of claim 27 based on Su in view of Kricka and did not restate the rejection, it appears that claim 27 is no longer rejected in light of this combination. However, on page 8 of the Office Action, the Examiner appears to believe the rejection still has merit. Therefore, to efficiently move this case forward, Applicants provide the following comments.

As described above, Su fails to disclose or suggest that a sperm type moves through an ion-permeable barrier and is separated from a sperm population through the ion-permeable barrier. Kricka is cited for fertilization of an ovum with viable sperm. Thus, the combination of Su and Kricka fails to disclose or suggest that a sperm type moves through an ion-permeable barrier and is separated from a sperm population through the ion-permeable barrier, which is required by claim 27. The Applicants, therefore, respectfully request that Examiner indicate allowability of claim 27 over this combination.

XI. 35 U.S.C. § 103(a) Engelmann in view of Weber in further view of Kricka.

Because the Examiner withdrew the rejection of claim 27 based on Engelmann in view of Weber in further view of Kricka and did not restate the rejection, it appears that claim 27 is no longer rejected in light of this combination. However, on page 8 of the Office Action, the Examiner appears to believe the rejection still has merit. Therefore, to efficiently move this case forward, Applicants provide the following comments.

Claim 27 ultimately depends from claim 1. As explained above, the results of claim 1, and therefore, of claim 27 are surprising and unexpected in light of Engelmann as modified by

Weber. Kricka is cited for its disclosure of fertilization of an ovum with viable sperm. The disclosure of Kricka does not make the results of claim 27 predictable in light of the Engelmann and Weber combination. The Applicants, therefore, respectfully request that Examiner indicate allowability of claim 27 over this combination.

XII. 35 U.S.C. § 112, first paragraph.

Claims 2 and 4 are rejected under 35 U.S.C. § 112, first paragraph. Although Applicants believe claims 2 and 4 are enabled in their rejected form, to expedite prosecution, these claims are amended herein. In particular, claim 2 is amended to delete genetic makeup or morphological normality. Claim 4 is amended to delete poor morphology, high levels of DNA damage, and high levels of oxygen species generation. The Examiner has indicated that the remaining scope of these claims is enabled. Applicants, therefore, respectfully request withdrawal of this rejection.

XIII. 35 U.S.C. § 112, second paragraph.

Claims 2 and 4 are rejected under 35 U.S.C. § 112, second paragraph for reciting sperm type having a desired genetic make up and morphological abnormality (claim 2), or an undesired high level of DNA damage and high levels of reactive oxygen species generation (claim 4). These listed characteristics have been deleted from claims 2 and 4 respectfully. Applicants, therefore, respectfully request withdrawal of this rejection.

XIV. Conclusions.

In view of the amendments and arguments herein, Applicants respectfully request allowance of all claims.

It is believed that all issues raised by the Examiner have been addressed. However, the absence of a reply to a specific rejection, issue, or comment does not signify agreement with or concession of that rejection, issue, or comment. In addition, because the arguments made above may not be exhaustive, there may be reasons for patentability of any or all pending claims (or

Applicant : Robert J. Aitken et al.
Serial No. : 10/574,911
Filed : May 11, 2007
Page : 20 of 20

Attorney's Docket No.: 10055-006US1

other claims) that have not been expressed. Finally, the amendment of any claim does not necessarily signify concession of unpatentability of the claim prior to its amendment.

Applicants wish to call the Examiner's attention to co-pending U.S. Patent Publication No. 2008/0067070 and encourage the Examiner to review this application and its corresponding file history.

Fees in the amount of \$555.00 for a three-month extension of time for a small entity are being paid concurrently herewith on the Electronic Filing System by way of Electronic Funds Transfer authorization. A Request for Continued Examination with its required fees are being filed concurrently with this Amendment. Please apply any other charges or credits to Deposit Account 50-5226.

Respectfully submitted,

Date: June 9, 2011

/Miles E. Hall/

Miles E. Hall, D.V.M.
Reg. No. 58,128

Customer Number 96039

Telephone: (404) 645-7700
Facsimile: (404) 645-7707

EXHIBIT A

TEXT

TheFreeDictionary Google Bing

AT

Search ?

New: Language forums

Like 11K

2 880 558 064 visitors served

Word / Article Starts with Ends with Text

Dictionary/thesaurus Medical dictionary Legal dictionary Financial dictionary Acronyms Idioms Encyclopedia Wikipedia encyclopedia ?

AT Also found in: [Medical](#), [Legal](#), [Financial](#), [Acronyms](#), [Encyclopedia](#), [Wikipedia](#), [Hutchinson](#)

0.01 sec.

[GE - Centricity Advance](#)

Ads by Google

See How EMR Software Can Make Your Medical Practice More Efficient.
GEhealthcare.com/CentricityAdvance[What is Cloud Computing?](#)Straight Talk about Cloud Computing from the Industry Leader. Get Info.
www.Microsoft.com/Cloud[Jos A Bank™ Official Site](#)Save 50% Off Suits, Dress Shirts & Ties! Ends 5/15. \$195+ Ships Free
www.JosBank.com

Page tools ?

[Printer friendly](#)[Cite / link](#)[Email](#)[Feedback](#)[Add definition](#)**AT**

abbr.

1. air temperature
2. also a/t antitank
3. automatic transmission

At¹

The symbol for the element astatine.

At²

abbr.

ampere-turn

aT

abbr.

attotesla



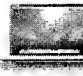

at¹ ¹

(ăt; ăt when unstressed)

prep.

1.
 - a. In or near the area occupied by; in or near the location of: *at the market; at our destination.*
 - b. In or near the position of: *always at my side; at the center of the page.*
2. To or toward the direction or location of, especially for a specific purpose: *Questions came at us from all sides.*
3. Present during; attending: *at the dance.*
4. Within the interval or span of: *at the dinner hour; at a glance.*
5. In the state or condition of: *at peace with one's conscience.*
6. In the activity or field of: *skilled at playing chess; good at math.*
7. To or using the rate, extent, or amount of, to the point of: *at 30 cents a pound; at high speed; at 20 paces; at 350°F.*
8. On, near, or by the time or age of: *at three o'clock; at 72 years of age.*
9. On account of, because of: *rejoice at a victory.*
10. By way of, through: *exited at the rear gate.*
11. In accord with; following: *at my request.*
12. Dependent upon: *at the mercy of the court.*
13. Occupied with: *at work.*

Idiom:**at it** *Informal*Engaged in verbal or physical conflict, arguing or fighting: *The neighbors are at it again.*[Middle English, from Old English *æt*; see *ad-* in Indo-European roots.]**at**² ² (ăt)

 <p>32 GB Apple iPad 3Gs Price: \$449 Bid: \$30.67 00:11 Save: 92%</p>	 <p>Apple iMac 27" 1TB Price: \$449 Bid: \$85.78 00:10 Save: 95%</p>
 <p>Apple MacBook Pro 15.4" 250 GB Price: \$449 Bid: \$65.84 00:10 Save: 75%</p>	 <p>Apple TV Black wi-fi Price: \$99 Bid: \$12.15 00:08 Save: 88%</p>

Department Stores are
Ripping you Off
Save up to 90% Off

Advertisement (Bad banner? Please [let us know](#))

Related Ads

- [Definition](#)
- [Define](#)
- [Define Blog](#)
- [TCP/IP Definition](#)
- [Legal Definition](#)
- [Add Definition](#)
- [Define Twitter](#)
- [Definition of HRA](#)
- [Dictionary Of](#)
- [Define Web 2.0](#)

My Word List ?

[Add current page to the list](#)


Samsung phones starting at **free** from AT&T

Shop Now

free shipping

the best deals are online

Advertisement (Bad banner? Please [let us know](#))

Charity ?



Feed a hungry child - donate to school feeding program

EXHIBIT B



Zeta potential of human X- and Y-bearing sperm

S. A. ISHIJIMA¹*, M. OKUNO¹, H. MOHRI² Issue

Article first published online: 16 MAY 2008

DOI: 10.1111/j.1365-2605.1991.tb01102.x



International Journal of
Andrology
Volume 14, Issue 5, pages
340–347, October 1991

Additional Information (Show All)

How to Cite Author Information Publication History

Abstract References Cited By

[Get PDF \(724K\)](#)

Keywords: human sperm; X-bearing sperm; Y-bearing sperm; zeta-potential

Summary

The zeta potential of human X- and Y-bearing sperm was measured by two different methods: (i) using an electrophoretic light scattering spectrophotometer, and (ii) using a laser-rotating prism. The X- and Y-bearing sperm were separated by free-flow electrophoresis, and their purities were determined by staining for the F-body using quinacrine mustard. The zeta potential of the sperm in the fraction containing more than 80% Y-bearing sperm was approximately -16 mV, whereas that of sperm in the fraction containing more than 95% X-bearing sperm was approximately -20 mV. In other words, the net negative-charge on the cell surface of human X-bearing sperm is higher than that of Y-bearing sperm.

[Get PDF \(724K\)](#)

More content like this

Find more content: [like this article](#)

Find more content written by: [S. A. ISHIJIMA](#) | [M. OKUNO](#) | [H. MOHRI](#) | [All Authors](#)



electrophoresis sperm x

Q Search



Zeta potential of human X- and Y-bearing sperm.
(PMID:1794918)

Ishijima SA, Okuno M, Mohri H

Department of Biology, College of Arts and Sciences, University of Tokyo, Japan.

International Journal of Andrology [1991, 14(5):340-7]

Type: Journal Article

DOI: 10.1111/j.1365-2605.1991.tb01102.x

Abstract

☐ Gene Ontology(1)

The zeta potential of human X- and Y-bearing sperm was measured by two different methods: (i) scattering spectrophotometer, and (ii) using a laser-rotating prism. The X- and Y-bearing sperm were determined by staining for the F-body using quinacrine mustard electrophoresis, and their purities were determined by staining for the F-body using quinacrine mustard. The fraction containing more than 80% Y-bearing sperm was approximately -16 mV, while the fraction containing more than 95% X-bearing sperm was approximately -20 mV. In other words, the cell surface of human X-bearing sperm is higher than that of Y-bearing sperm.

Read Article at **WileyInterScience** (Subscription required)

How does UK f

Cited By - displaying 3 of 3 citations • Web of Science
(9)- subscription required



Retention of membrane charge attributes by cryopreserved-thawed sperm and zeta selection.
(PMID:17653847)



Selection of sperm based on combined density gradient and Zeta method may improve ICSI outcome.
(PMID:19553239)



Evaluation of zeta and HA-binding methods for selection of spermatozoa with normal morphology, protamine.
(PMID:20078511)

Cites the following - displaying 16 of 16 citations

Title not supplied - full information unavailable
bangham
proceedings of the royal society of london [1961]

EXHIBIT C

Sperm Motility Under Conditions of Weightlessness

UTE ENGELMANN,* FRANZ KRASSNIGG,† WOLF-BERNHARD SCHILL*

From *the Department of Dermatology and Andrology, Justus Liebig University Giessen, Giessen, Germany, and †the Austrian Federal Environmental Agency, Salzburg, Austria.

ABSTRACT: The aim of this study was to determine the differences in motility of frozen and thawed bull spermatozoa under conditions of weightlessness compared with ground conditions. The tests were performed within a series of scientific and technologic experiments under microgravity using sounding rockets in the Technologische Experimente unter Schwerelosigkeit (TEXUS) program launched in Kiruna, North Sweden. Using a computerized sperm motility analyzer, significant differences were found in sperm motility under microgravity compared with sperm under gravitational conditions on earth. Computer anal-

ysis showed alterations in straight line and curvilinear velocity, as well as in linearity values. The amount of progressively motile spermatozoa, including all spermatozoa with a velocity $> 20 \mu\text{m}/\text{second}$, increased significantly from $24\% \pm 9.5\%$ in the reference test to $49\% \pm 7.6\%$ in the microgravity test. In conclusion, there is strong evidence that gravity influences sperm motility.

Key words: sperm motility, weightlessness.
J Androl 1992;13:433-436.

Several studies have shown that some processes take place differently and more favorably under zero gravity than under terrestrial gravitational conditions. Consequently, certain properties can only be achieved under these conditions. In this study, the motility of frozen and thawed bull spermatozoa was investigated under conditions of weightlessness and compared with motility under normal conditions on earth. Thus, the influence of gravity on functional processes of higher biologic systems was studied.

For many reasons, the spermatozoon is an ideal model for examination of physiologic functions. So far, it is still unknown to what extent and in which manner biologic processes like cell differentiation, transportation, and development are influenced by gravity. Therefore, investigations performed under conditions of zero gravity should contribute to the understanding of the influence of gravity on molecular mechanisms involved in basic biologic functions. In this investigation, the effect of gravity on sperm movement characteristics was clearly demonstrated. As a result of the great attention during recent years to the objective analysis of sperm motility, it has become increasingly apparent that progressively motile spermatozoa and their movement characteristics are of biologic and, hence, clinical importance.

Supported in part by grants from the German Federal Ministry of Research and Technology (contract number QV 87010).

Correspondence to: W.-B. Schill, Department of Dermatology and Andrology, Justus Liebig University Giessen, Gaffkystrasse 14, D-6300 Giessen, Germany.

Received for publication September 25, 1991; accepted for publication April 3, 1992.

Materials and Methods

Material

Semen samples were obtained from bulls of the animal breeding and insemination station in Grub, Germany. Ejaculates were collected using an artificial vagina. Samples showing at least 80% sperm motility were diluted to a concentration of 40 to $50 \times 10^6/\text{ml}$ and frozen in 0.5-ml straws according to the method of Steinbach and Foote (1967). Frozen samples were thawed and maintained at 39°C until examination.

Experimental Design and Mission Performance

Experiments were carried out as part of the Technologische Experimente unter Schwerelosigkeit (technological experiments under microgravity; TEXUS) program in November, 1988 (TEXUS 19) and in May, 1990 (TEXUS 26) within a series of other scientific and technologic experiments under microgravity conditions using sounding rockets (Skylark VII, British Aerospace Corporation). The TEXUS program, which is dedicated to the preparation of scientific experiments on board Spacelab, was initiated in 1976. TEXUS encompasses an unmanned German government rocket program that ensures weightlessness conditions for about 360 seconds and transports a payload of about 300 kg to an altitude of 250 km. The payload is recovered by parachute and returned to the launch site by helicopter. The launch campaign is carried out in Kiruna, North Sweden, in cooperation with the European Space Agency (ESA) and the Swedish Space Corporation (SSC).

Samples were measured in a specially developed, air-tight and temperature constant (39°C) chamber (Strömberg-Mika, Bad Feilnbach, Germany), which was part of the TEXUS module (Fig. 1). Thawed spermatozoa were observed under a negative phase-contrast microscope (objective, Nikon ELWD 20x; ocular, Nikon

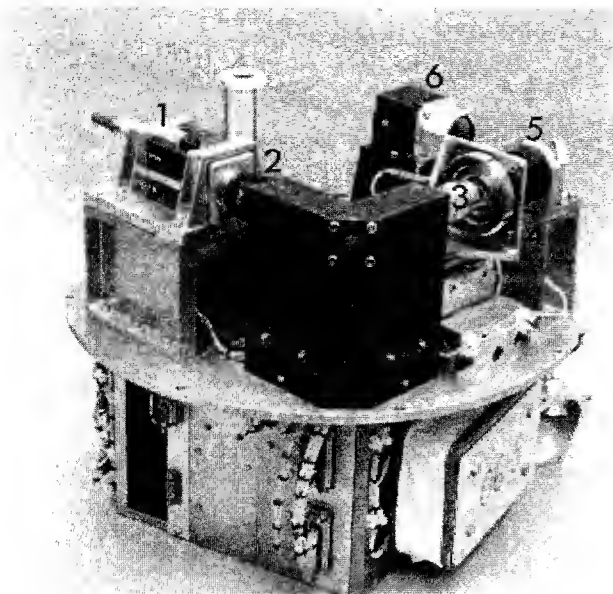


FIG. 1. The TEXUS experiment module. The module shown in the figure was developed by MBB-ERNO (Bremen, Germany). It was equipped with (1) a camera system (CCD); (2) ocular (Nikon CFW 15 \times); (3) objective (Nikon ELWD 20 \times); (4) chamber; (5) condenser, filter, deflecting mirror; and (6) lamp casing.

CFW 15 \times ; Nikon Corporation, Tokyo, Japan). About 40 minutes before launching, samples were integrated into the payload. After lift-off, semen cells in the chamber could be monitored directly on line with a television camera. The observer on the ground was able to influence and to control experimental parameters via telecommand channels so that sharpness of focus could be adjusted. Another channel allowed 12 (TEXUS 19) and 17 (TEXUS 26) different fields of vision during the microgravity phase. The television pictures were recorded on the ground. The actual gravitational force during the time of observation was $< 10^{-4} g$.

Video tapes were evaluated using a computerized semen motility analyzer (SM-CMA; Strömberg-Mika, Bad Feilnbach, Germany), which enabled the measurement of total and progressive sperm motility, as well as determination of sperm velocity (Katz et al, 1985, 1987; Knuth et al, 1987; Mortimer et al, 1988). The frame rate for motility analysis was 25 Hz. The time between two successive video frames was 40 msec; the actual observation time for each spermatozoon was 600 msec. Only those cells that could be detected in eight successive frames were evaluated. Curvilinear velocity was calculated from the sum of the straight line distances between all points along the track. Straight line velocity was calculated from the straight line distances between the first and last point of the track. In addition, within the group of progressively motile spermatozoa, three classifications could be distinguished, characterizing the quality of motion (Auger and Dadoune, 1988) by calculation of the linearity values (ratio of straight line to curvilinear, S/V ; Fig. 2).

To compare the data obtained during the flight of TEXUS 19, the motility of another aliquot of the same ejaculate was examined under identical conditions on the ground. In the TEXUS 26 experiment, the reference test was carried out immediately before the

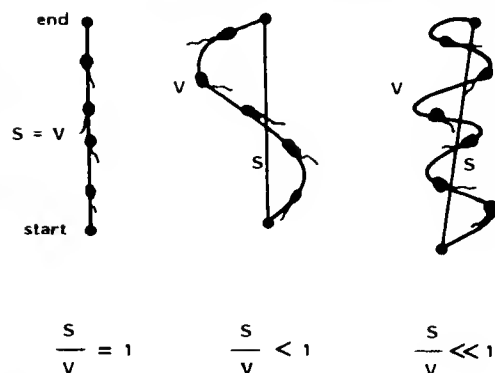


FIG. 2. Examples of motion patterns of spermatozoa. Motility characteristics were derived from video acquisition and processing of the sperm track. V = curvilinear velocity ($\mu\text{m}/\text{sec}$); S = straight line velocity ($\mu\text{m}/\text{sec}$), showing different moving patterns within groups of progressively motile spermatozoa. Progressively motile spermatozoa are split into three groups in accordance with their S/V ratios: $S/V = 0.9$ to 1.0 = linear forward; $S/V = 0.8$ to 0.9 = not linear forward; $S/V = 0.0$ to 0.8 = other movement pattern.

launch using the same sample that was to be observed under microgravity. The advantage of using the same sample was the elimination of variations within the measurements normally found in different aliquots of the same ejaculate. In TEXUS 19, a total of 761 and 698 spermatozoa were evaluated under $1 g$ and zero g , respectively. By increasing the fields of vision, a total of 1154 and 1090 spermatozoa could be observed in TEXUS 26. The Wilcoxon signed rank test was used for analysis of significance.

Results

In TEXUS 19, no differences in quantitative sperm motility (which refers to velocity) were detectable under conditions of weightlessness when compared with motility under gravitational conditions on earth. Total motility and the percentage of spermatozoa with progressive motility (velocity $> 20 \mu\text{m}/\text{sec}$) were nearly identical under $1 g$ and microgravity conditions (Fig. 3). However, computer analyses showed significant alterations in motility patterns, which signify changes in path shape and are expressed as linearity value. The amount of linear forwardly motile spermatozoa (linearity value > 0.9) rose significantly (Fig. 4) from $42\% \pm 9\%$ in the reference test on the ground to $73\% \pm 8\%$ in the microgravity test ($P < 0.005$). On the other hand, there were no significant differences in straight line or curvilinear velocity. For both samples, there were only small deviations between velocity values under conditions of weightlessness and values for the reference sample on earth (Table 1). But these small differences were sufficient to shift the S/V ratio so that the portion of linearly moving spermatozoa rose significantly.

In TEXUS 26, total motility was $71.4\% \pm 7.2\%$ in the reference test and $79\% \pm 6.2\%$ under microgravity condi-

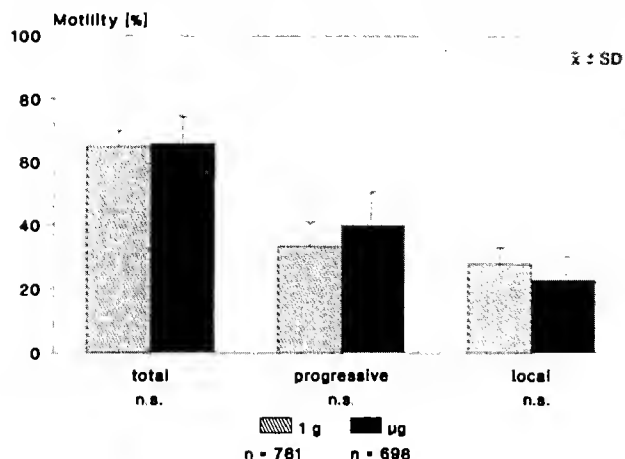


FIG. 3. Comparison of quantitative motility on the ground (1 g) and under conditions of weightlessness (microgravity) in TEXUS 19. Spermatozoa are classified into three groups according to their velocity values: (a) total motility = all spermatozoa that move at a velocity $>10 \mu\text{m/sec}$; (b) progressive motility = all spermatozoa that move forward at a velocity $>20 \mu\text{m/sec}$; (c) local motility = all spermatozoa that move within a range of $10 \mu\text{m/sec}$ and $20 \mu\text{m/sec}$. n.s. = not significant.

tions ($P < 0.005$). A statistically high significant difference could be observed in the group of progressively motile spermatozoa (Fig. 5). Progressive motility increased from $23.9\% \pm 9.5\%$ at ground conditions to $49\% \pm 7.6\%$ ($p < 0.005$) during flight. Curvilinear velocity values within this group also rose significantly, from $28.8 \mu\text{m/sec} \pm 2.5 \mu\text{m/sec}$ on earth to $31.9 \mu\text{m/sec} \pm 3.2 \mu\text{m/sec}$ in space ($P < 0.01$; Table 1). At the same time, local motility decreased from $47.5\% \pm 9.1\%$ in the reference test to $30\% \pm 6.5\%$ in

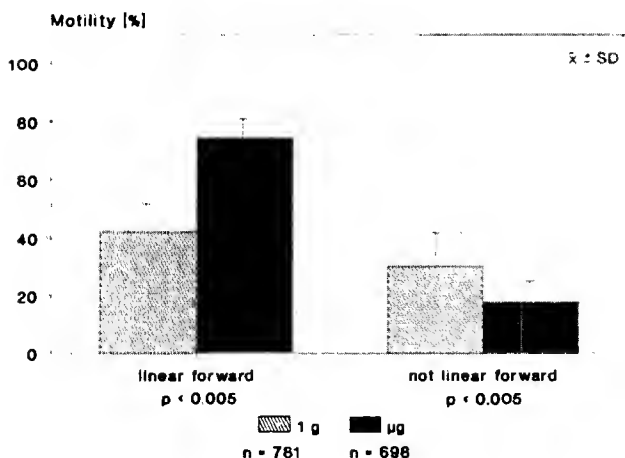


FIG. 4. Motion patterns of progressively motile spermatozoa on the ground compared with those under conditions of weightlessness in TEXUS 19. Path shape is characterized and expressed by means of the S/V ratios = linearity values. These are defined as shown in Figure 2.

Table 1. Velocity data from bull spermatozoa on earth and under conditions of weightlessness

	TEXUS 19		TEXUS 26	
	Microgravity	1 g	Microgravity	1 g
Velocity (S)	29.1 ± 9.4	27.5 ± 6.2	26.9 ± 2.8	23.8 $\pm 2.5^*$
Velocity (V)	29.8 ± 9.9	30.9 ± 7.5	31.9 ± 3.2	28.8 $\pm 2.5^\dagger$

S = straight line velocity in $\mu\text{m/sec}$, V = curvilinear velocity in $\mu\text{m/sec}$.

* $P < 0.005$.

† $P < 0.01$.

the microgravity test ($P < 0.005$; Fig. 5). This implies that 17.5% of the so-called local motile spermatozoa, which are defined as cells with velocity values between $10 \mu\text{m/sec}$ and $20 \mu\text{m/sec}$, could overcome the theoretically fixed velocity borderline of $20 \mu\text{m/sec}$. Under the influence of weightlessness, these cells could be classified by computer analysis as progressively motile spermatozoa. Regarding qualitative motility patterns (path shape), the portion of linear forwardly motile spermatozoa with linearity values >0.9 rose significantly from $30.5\% \pm 12.8\%$ on the ground to $42.2\% \pm 16.1\%$ ($P < 0.01$) during flight (Fig. 6). This means there was an increase of linearity of 12% under the influence of weightlessness.

Discussion

Using bull spermatozoa, it was possible for the first time to show the influence of gravity on the motility of biologic

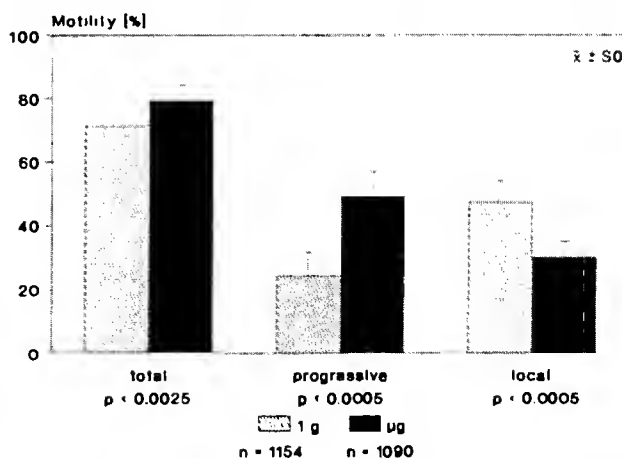


FIG. 5. Comparison of quantitative motility on the ground (1 g) and under conditions of weightlessness (microgravity) in TEXUS 26. Spermatozoa are classified into three groups according to their velocity values: (a) total motility = all spermatozoa that move at a velocity $>10 \mu\text{m/sec}$; (b) progressive motility = all spermatozoa that move forward at a velocity $>20 \mu\text{m/sec}$; (c) local motility = all spermatozoa that move within a range of $10 \mu\text{m/sec}$ and $20 \mu\text{m/sec}$.

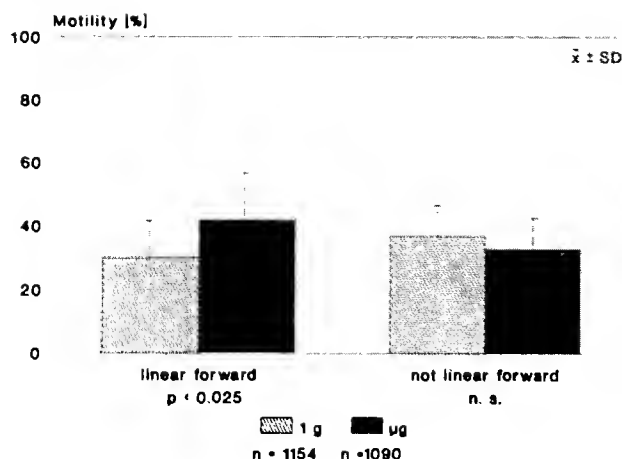


FIG. 6. Motion patterns of progressively motile spermatozoa on the ground compared with those under conditions of weightlessness in TEXUS 26. Path shape is characterized and expressed by means of the S/V ratios = linearity values. These are defined as shown in Figure 2. n.s. = not significant.

systems. In the TEXUS 19 experiment, the first indications of the effects of microgravity were detectable, which were confirmed after the reflight of TEXUS 26. Reasons for the differences in the results found in both experiments can be attributed to the better experimental conditions during the second flight test. The use of the same ejaculate sample for both the reference test under terrestrial conditions and the microgravity test was very advantageous. In the first TEXUS 19 experiment, the reference test was carried out by thawing another sample of the same ejaculate.

The changes detected in motility characteristics are definitely due to weightlessness, as the results of the experiments demonstrate. This could also be proven by a series of supporting ground experiments in which launching conditions, like acceleration (12 g) and vibration, were simulated. No change in sperm movement properties was detectable in any case. Thus, microgravity conditions favor the motility pattern of spermatozoa and might possibly improve their fertilization capacity.

There are possible explanations for these effects of microgravity on sperm motility characteristics. The enhancement may be due to changes in membrane permeability, energy balance, or both. It also might be that in microgravity, energy supplying mechanisms function more economically and more rapidly. The activity of membrane-bound enzymes like thymidine kinase (E.C. 2.7.1.21) might be influenced by microgravity-induced changes of membrane permeability, causing an effect on DNA synthesis (Tairbekov et al, 1982). The results of other space missions substantiate these assumptions, proving that weightlessness can have an influence at the cellular level.

The Cytos Franco-Soviet experiments made on a unicellular organism, the paramecium, on board Salyut 6 have shown a strong stimulating effect on cell growth rate (Planel et al, 1981). Among other effects, an increase in cytoplasmic hydration, a drop in total protein content, and a change of the electrolytic content were found. This was shown by a decrease in intracellular calcium, probably related to structural changes in the cytoskeleton proteins, especially in their sites for calcium binding, or to modifications of the energetic metabolism connected to ciliary movement (Tixador et al, 1981).

Montgomery et al (1978) reported that embryonal lung cells (WI-38) cultivated under microgravity conditions showed a 20% reduction in glucose consumption compared with cells tested in ground-based experiments. This suggests that energy consumption was lower for cells cultured in the absence of gravity than for cells kept in the ground laboratory. On the basis of these findings and the results of the TEXUS experiments, it would be of great interest to extend these studies to other biologic systems, especially to primate cells.

Acknowledgments

The authors thank Dr. O. Haeger, of the Test and Insemination Station in Grub (Germany), for providing bull spermatozoa, and Mrs. A. Full for her expert technical assistance.

References

- Auger J, Dadoune JP. Computerized sperm motility and application of sperm cryopreservation. *Arch Androl.* 1988;20:103-112.
- Katz DF, Davis RO, Delandmeter BA, Oversireet JW. Real-time analysis of sperm motion using automatic video image digitization. *Comput Methods Programs Biomed.* 1985;21:173-176.
- Katz DF, Davis RO. Automatic analysis of human sperm motion. *J Androl.* 1987;8:170-181.
- Knuth UA, Yeung C-H, Nieschlag E. Computerized semen analysis: objective measurement of semen characteristics is biased by subjective parameter setting. *Fertil Steril.* 1987;48:118-124.
- Montgomery POB Jr., Cook JE, Reynolds RC, et al. The response of single human cells to zero gravity. *In Vitro.* 1978;14:165-173.
- Mortimer D, Serres C, Mortimer ST, Jouannet P. Influence of image sampling frequency on the perceived movement characteristics of progressively motile human spermatozoa. *Gamete Res.* 1988;20:313-327.
- Planel H, Tixador R, Nefedov Y, et al. Space flight effects on Paramecium tetraurelia flown aboard Salyut 6 in Cytos 1 and Cytos M experiments. *Adv Space Res.* 1981;1:95-100.
- Steinbach I, Foote RH. Osmotic pressure and pH effects on survival of frozen bovine spermatozoa. *J Dairy Sci.* 1967;50:205-213.
- Tairbekov M, Voronkov LA, Gzova A. Some physical and biochemical features of cells of carrot gall developed in weightlessness. *Space Biol Aerospace Med.* 1982;16:62-67.
- Tixador R, Richoille G, Templier J, Monrozier E, Maotti M, Planel H. Etudes de la teneur intra et extracellulaire des électrolytes dans les cultures de paramecies réalisées pendant un vol spatial. *Biochim Biophys Acta.* 1981;649:175-178.

EXHIBIT D

Marcella Chiari¹
Luca D'Alesio¹
Roberto Consonni²
Pier Giorgio Righetti³

¹Istituto di Chimica degli Ormoni,
CNR, Milano

²Istituto di Chimica delle
Macromolecole, NMR lab, CNR,
Milano

³Department of Cell Biology,
University of Calabria in Arcavacata
di Rende, Cosenza

New types of large-pore polyacrylamide-agarose mixed-bed matrices for DNA electrophoresis: Pore size estimation from Ferguson plots of DNA fragments

The average pore size value of gels containing polyacrylamide, covalently linked to agarose, was found to be 30% higher than the value of a regular *N,N'*-methylenebisacrylamide (Bis) cross-linked gel of the same %T. By increasing the agarose concentration (10% of the total amount of polyacrylamide), gels containing low amounts of acrylamide (1.5–2%) are reproducibly obtained; their pore sizes are 130% larger than the pore sizes of a 4%T, 3.3%C polyacrylamide gel. In general, mixed-bed matrices were found to be more elastic and mechanically stronger than classical polyacrylamide gels since an agarose-induced gelation process takes place during their polymerization.

1 Introduction

The ability to separate and recover DNA is a key component in studies of genetic regulation, genomic sequence, diagnostic analysis and disease. Restriction mapping of genomic DNA and analysis of PCR products require the electrophoretic separation of DNA fragments ranging in size from a few hundred to several million base pairs (bp), while DNA sequencing requires a separation method capable of resolving fragments differing by a single nucleotide in length. The most frequently used matrices in slab-gel electrophoresis are cross-linked polyacrylamide and agarose. Depending on the monomer and cross-linker concentration, pores of 5–25 nm are typically produced for polyacrylamide gels [1] whereas gelation of agarose leads to pore sizes of about 50–200 nm or higher [2]. This large pore size of agarose gels results from its ability to form helices, which laterally aggregate into pillar-like structures. Cross-linked polyacrylamide is employed for the separation of molecules with M_r of up to a few hundred thousand, whereas agarose is used for separations beyond this range. Agarose is the matrix of choice for the electrophoresis of high molecular mass DNA while its use, in the field of proteins, is limited to large molecules like lipoproteins, proteoglycans and immunoglobulins. Polyacrylamide is widely employed for protein separations because its average pore size is close to the average diameter of globular proteins; moreover, the small size of its pores provides a tool for DNA sequencing and line mapping.

Matrices of intermediate pore sizes between that of acrylamide and the agarose would be extremely useful in the separations of biopolymers because there are important areas of interest in the field of protein and DNA analysis in which the two most common matrices fail for different reasons. The resolution of DNA fragments in the range of 1000–5000 bp is not linear in polyacrylamide gels whereas the sieving capability of agarose is inadequate and the bands in this region are too dif-

fuse. The resolution of higher molecular mass proteins is incomplete in standard polyacrylamide gels because of their poor gel penetration; this analysis requires highly porous, low-concentration polyacrylamide gels, which are difficult to handle, while agarose does not offer enough sieving capability. An improvement of DNA sequencing techniques can also be linked to the availability of new gels with larger pores.

In the past 10 years some articles have reported the use of new matrices which are based on substituted acrylamido monomers, none of which, from our point of view, has dealt in the proper way with the porosity problem. Boschetti [3] proposed a new monomer, Trisacryl, containing a 2-hydroxymethyl-2-propanediol residue linked to the nitrogen of the amido group of acrylamide. Even though the matrix has a suitable hydrophilic character that reduces the interactions with proteins, and a larger porosity due to the monomer's higher M_r value, unfortunately this support has not found applications as a continuous matrix in electrophoresis because of its inherent instability. As demonstrated by Chiari *et al.* [4], the presence of –OH groups in the alkyl-substituent of the nitrogen of the monomer lessens the hydrophobicity of the resulting polymer; however, such –OH groups should be kept at a distance from the amido group suitable to prevent the formation of rings with 5, 6 or 7 members containing the amido linkage. The elongation of the chain substituent carrying the OH prevents the transfer [5] of the acryloyl residue from the N to the O and avoids the intramolecular formation of an ester bond which is rapidly hydrolyzed, producing acrylic acid. Another electrophoretic support, Hydrolink [6], developed specifically for DNA separations, was described in 1989. Hydrolink materials represent a novel family of gels based on *N*-disubstituted acrylamidomonomers. Their porosity is described to be intermediate between those of polyacrylamide and agarose gels. Due to its character, the matrix seems to provide linear resolution from 100 to 5000 bp. However, the hydrophobicity of alkyl-substituted acrylamides in the matrix is too high to be useful for protein analysis, while another drawback is that the methacrylate cross-linkers, present in Hydrolink formulations, are prone to hydrolysis.

More recently we have proposed [4] a new monomer, *N*-acryloylaminoethoxyethanol (AAEE), combining high hydrophilicity with hydrolytic stability. The gels formed

Correspondence: Dr. Marcella Chiari, Istituto di Chimica degli Ormoni, via Mario Bianco 9, CNR, 20131 Milano, Italy (Tel: +02-284-7737; Fax: +02-284-1934)

Nonstandard abbreviation: TAE, Tris-acetate-EDTA

Keywords: Polyacrylamide / Agarose / Mixed matrices / DNA electrophoresis

by this monomer show a strong resistance to alkaline hydrolysis and their porosity appears to be larger compared to polyacrylamide of the same %T value, since the M_n of AAEE is double that of acrylamide. Poly(AAEE) formulations represent a solution to the problems of hydrolytic instability and the mobility of DNA fragments is about 10–15% higher than the mobility in the corresponding polyacrylamide gels. In another approach, Righetti *et al.* [7] described "laterally aggregated" polyacrylamide gels for electrophoresis. These new, highly porous matrices are obtained from a standard mixture of monomers (5%T, 4.4%T) polymerized in presence of polyethylene glycol (PEG, 10 kDa) which induces lateral chain aggregation, causing an interchain hydrogen bond formation. The porosity of this type of gel was estimated by electron microscopy and it was found to be of the order of 2–300 nm. Laterally aggregated polyacrylamide gels are routinely used in chromatography for producing discontinuous matrices but their use in electrophoresis is still in its infancy [8].

It is well known that an increase in pore size is achieved by increasing the cross-linker concentration [9] or decreasing the % of the monomers [10]. However, this type of gels lacks mechanical strength, and in some cases they extrude water and are, in general, difficult to handle. Pore size of polyacrylamide gels is inversely related to its concentration, but polyacrylamide does not form gels below a concentration of 2% [11]. In order to overcome this problem, cross-linked acrylamide is polymerized in the presence of agarose, thus forming stable gels with 0.5–1.5% acrylamide and 0.6% agarose. The agarose-polyacrylamide gel electrophoresis procedure was originally used for the analysis of proteoglycans, large proteins with molecular masses greater than 2.5 million Da [12]. The structures obtained at such low polyacrylamide concentrations are sufficiently porous to allow penetration of the very large proteoglycans. The composite gels, consisting of different combinations of acrylamide and agarose, allow reduction of the acrylamide concentration still offering favorable mechanical properties: they have been used for analysis of nucleic acids [13], viruses [14] and SDS-denatured, high molecular mass apolipoproteins [15]. Various types of formulations were tried in order to produce large-porosity composite gels: matrices of discontinuous buffer composition [16] and exponential gradient gels, from 0 to 10% acrylamide, and constant % agarose were used for the separation of large lipoproteins [17].

In 1984 mixed-bed acrylamide-agarose gels, lacking covalent cross-linking with methylene bisacrylamide were introduced for separations of proteins and nucleic acids [18]. The gels obtained are thermo-reversible with a melting point at 85 °C. High concentrations of linear polyacrylamide (from 10 to 15%) polymerized in presence of agarose (from 1 to 2%), produce gels which offer separations of proteins and DNA comparable with those obtained from standard *N,N*-methylenebisacrylamide cross-linked gels. Noncross-linked polymer matrices for electrophoretic separations by sieving were described by Bode [19] and Tietz *et al.* [20] who found that polymer concentrations lower than 10%T could not be maintained on the slab gel. The linear gels are commonly

used as sieving matrices in capillary electrophoresis at concentrations lower than 10% because of the anticonvective nature of a capillary. Low-concentration polymer networks show the ability to resolve, in a single capillary zone electrophoresis (CZE) run, both small and large DNA fragments [21] (up to 23000 bp were analyzed in this system).

The present paper describes the characteristics of new types of mixed-bed matrices formed by copolymerization of allylglycidyl-derivatized agarose and acrylamide. Ethylenically unsaturated polysaccharide resins containing isolated carbon-carbon double bonds, which undergo addition by polymerization or copolymerization in the presence of a catalyst, have been previously described [22]. Their use was limited to the production of electrophoretic supports in the form of gel films, with improved drying characteristics, useful in the separation of proteins. The aim of the present work was to investigate the porosity of the agarose-acrylamide gels, using the electrophoretic migration of double-stranded DNA molecules as a model. The mechanical properties of these composite gels are favorable also when working at a low concentration of acrylamide: easy gels to handle are formed at concentrations of polyacrylamide as low as 1.5–2%. The porosity of these formulations appears to be controlled by the polyacrylamide concentration used, whereas the amount of agarose plays a role on the mechanical properties of the gels but its influence on the pore size is limited.

2 Materials and methods

2.1 Gel media

Agarose (LE), acrylamide, *N,N*-methylenebisacrylamide (Bis), ammonium persulfate (AP) and *N,N,N',N'*-tetramethylethylenediamine (TEMED) were purchased from Bio-Rad (Hercules CA, USA); allylglycidyl ether was from Aldrich (Milwaukee, WI, USA); Tris(hydroxymethyl)aminomethane, boric acid, and ethylenediaminetetraacetic acid (EDTA) were purchased from Sigma (St. Louis, MO, USA).

2.2 DNA samples

The following DNA molecular mass markers: marker V, a mixture of fragments from cleavage of plasmid pBR322 with restriction endonuclease *Hae*III, marker VI, a mixture of fragments from cleavage of plasmid pBR328 with restriction endonuclease *Bgl*I and of pBR328 with *Hinf*I, and marker III, a mixture of fragments from cleavage of lambda-DNA endonucleases, were from Boehringer Mannheim (Germany); the 1 kbp ladder was from Bethesda Research Labs (Gaithersburg, MO, USA).

2.3 Activation of agarose

Thirty three mg of sodium borohydride and 1.6 mL of allylglycidyl ether were added, under magnetic stirring, to a suspension of agarose (1 g) in NaOH (33 mL, 0.3 M). After stirring for 12 h, agarose was recovered from the suspension by filtration and washed with distilled water

to neutral pH. The derivatized agarose was dehydrated with methanol and dried in an oven at 35°C under vacuum.

2.4 Nuclear magnetic analysis

Activated agarose was dissolved in DMSO- d_6 at 90°C. After complete solubilization the temperature was lowered to 50°C and all the ^{13}C spectra at 50.29 MHz were acquired on the AM-Bruker wide-bore spectrometer.

2.5 Preparation of polyacrylamide gels

For all experiments reported here, $15 \times 16 \times 0.8$ cm slab gels, cast between glass plates, were used. The gels were run in a Protean II 2-D cell purchased from Bio-Rad. A stock solution (30%T, 3.3%C, where T represents the total amount of monomers) was diluted to the proper concentration of acrylamide and Bis with $1 \times$ Tris-acetate-EDTA (TAE) buffer (40 mM Tris, 20 mM acetic acid, 1 mM EDTA, pH 8.2), then 1 μL per mL of TEMED and 1 μL per mL of ammonium persulfate (from a stock at 40%) were added, and the solution was mixed and quickly poured into the previously prepared gel cassette. Gelation usually occurred within 5–10 min, depending on the acrylamide concentration. Each gel was polymerized overnight in order to allow the polymerization reaction to proceed to near completion.

2.6 Preparation of agarose-acrylamide hybrid gels

For all experiments reported here, $15 \times 16 \times 0.8$ cm slab gels cast between glass plates as described in paragraph 2.5 were used. The desired amount of a mixture of activated agarose and normal agarose (ratio 2:1) was dissolved at 95°C in $1 \times$ TAE, the solution was cooled at 50°C under stirring, the desired amount of acrylamide was then added and the volume was adjusted to its final value; then 0.3 μL per mL of TEMED and 0.8 μL per mL of ammonium persulfate (from a stock at 40%) were added, and the solution was mixed and quickly poured into the previously prepared gel mold. Gelation usually occurred within 5–10 min, depending on the acrylamide concentration. In this case the polymerization reaction was also allowed to proceed overnight. The polyacrylamide concentration in each gel is indicated as %T whereas the percentage of agarose is in some cases stated as w/v concentration (g of agarose per 100 mL of gel) and in some others as w/w (g of agarose over g of polyacrylamide in 100 mL).

2.7 Electrophoresis

Electrophoresis was carried out in a vertical slab gel apparatus. The electric field was supplied by a Pharmacia LKB ECPS 3000/150 regulated power supply. The applied voltage was always 150 V, corresponding to an effective field strength in the gel of 10 V/cm (from the applied voltage and the distance between the electrodes). All gels were run at a controlled temperature of 23°C. Four μL of samples containing 250 $\mu\text{g}/\text{mL}$ of DNA were typically loaded in 3×5 mm sample wells; each solu-

tion also contained 0.8 μL of a solution containing 1 $\mu\text{g}/\text{mL}$ bromophenol blue marker dye in 50% glycerol. The duration of electrophoresis ranged from 1 to 4 h, depending on the composition of the gel; all gels were run until the marker dye had migrated 70% of the length of the gel. After electrophoresis, the gels were stained 15 min in a solution containing 2.5 $\mu\text{g}/\text{L}$ ethidium bromide. Mobilities were determined from photographs of the stained gels by using the measurement of a ruler photographed simultaneously to provide the magnification factor.

2.8 Calculation of absolute mobilities

The apparent mobility of the various DNA restriction fragments was calculated from Eq. (1).

$$\mu_{\text{app}} = d/Et \quad (1)$$

where μ_{abs} is the absolute mobility, d is the distance in cm migrated by a given fragment in the gel, E is the electric field strength in V/cm, and t is the time in seconds. The absolute mobility calculated from fragments in gels of identical compositions agreed within $\pm 5\%$.

2.9 Calculation of Ferguson plots

For each of the DNA fragments ranging from 64 to 1330 bp of the different DNA markers, Ferguson plots were constructed by plotting the logarithm of the absolute mobility of the fragment as a function of gel concentration, %T. They y-axis intercepts of the straight lines, extrapolated from the experimental values of the Ferguson plots to zero gel concentration, represent the μ_0 .

2.10 Estimation of gel pore size from the Ferguson plots

According to the Ogston theory [23] when the DNA fragment has a size M (in kbp) and length L such that $R_m \leq \bar{a}$, where \bar{a} is the average pore size of the gel, the gel is thought to separate the different fragments by a sieving mechanism [24]. In this case, the curves μ_{abs} vs. %T can give an estimation of the average pore size a as a function of the matrix concentration. Ferguson plots [25] can be used to estimate the effective pore size of polyacrylamide gels by determining the gel concentration at which the mobility of a given DNA fragment is equal to half its mobility at zero gel concentration. At this gel concentration, assuming a Gaussian distribution of pore sizes, a macromolecule with a size equal to the median pore radius of the gel should be able to access half the available gel volume [9, 23, 24, 26–29]. The most appropriate value for the radius of the DNA migrating macromolecules that has to be used is an object of debate. In the present work, according to [26], the geometric mean radius, \bar{R} , the radius of a sphere equal in volume to the cylindrical DNA molecule [30, 31], was used to estimate DNA size. For DNA the geometric mean radius \bar{R} , in nm, is defined as:

$$\bar{R} = 0.755 (\text{bp})^{1/3} \quad (2)$$

where bp is the number of bp in the fragment.

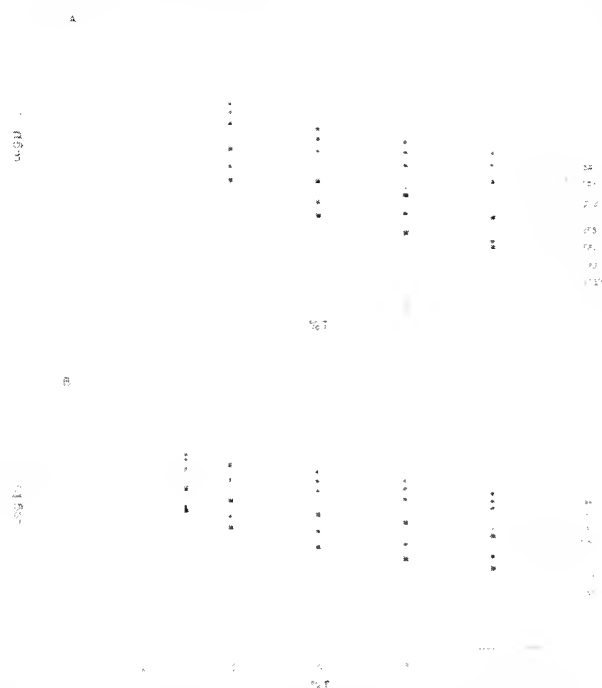


Figure 4. Ferguson plots based on absolute mobility. The logarithm of the absolute mobility, μ_0 , is plotted as a function of polyacrylamide concentration, %T (A) in 3.3% Bis cross-linked gels, and (B) in hybrid gels. The number of base pairs is indicated beside each curve. The straight lines represent linear regression of the experimental values indicated in the plots.

and they are both linear and nearly parallel. The increase of their slopes, with DNA molecular mass, is slower for mixed-bed gels than for polyacrylamide gels. Both Ferguson plots do not appear to converge at a common intercept at zero gel concentration. As described by Holmes and Stellwagen [33, 34], the Ferguson plot profiles are determined by the cross-linker concentration: gels containing 0.5–3%C show parallel curves, whereas gels containing 4% Bis appear to converge close to a common intercept at zero gel concentration. The mobility in low cross-linked gels decreases slowly while increasing the gel concentration and fragment size.

3.2 Mobility at zero gel concentration

The mobility in free solution [35] should be independent of DNA molecular mass; its value is a function of temperature and ionic strength. However, according to other authors [34], the absolute mobility, extrapolated at zero gel concentration from the experimental Ferguson plots, depends on the size of the DNA fragment considered and on the gel composition since the different curves do not intercept the x axis at the same value. The μ_0 (Y value in the terminology of Rodbard and Chrambach [24, 36]) cannot be directly extrapolated from the Ferguson plot. To determine the μ_0 , the mobility of the smaller DNA marker fragments was extrapolated to zero gel concentration, and to zero molecular mass as shown in Fig. 5a for the mixed-bed gels and in Fig. 5b for the polyacrylamide gels. The necessity of extrapolating the free mobility from a double-limits plot suggests that an inter-

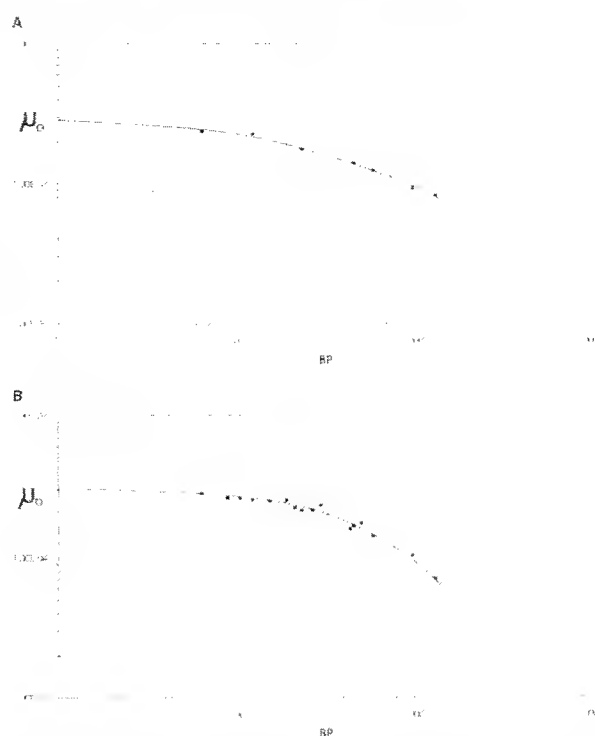


Figure 5. Log-log plots of the absolute mobility extrapolated to zero gel concentration, μ_0 , as a function of the number of base pairs in the fragment. Values extrapolated from Ferguson plots of Fig. 4: (A) Polyacrylamide gels, (B) hybrid gels.

action between the DNA molecules and the electrophoretic support occurs during electrophoresis. The estimated μ_0 value was of 2.8×10^{-4} for the mixed-bed gels and 3.0×10^{-4} for the polyacrylamide gels. Both these values are lower compared with the values determined in free solution and reported in the literature [30]. The values extrapolated from the experimental curves were used to determine the size of the fragments of mobility corresponding to $\mu_0/2$.

3.3 Gel pore radius determination for polyacrylamide and mixed-bed gels

The pore size of polyacrylamide gels containing 3%C was determined by Holmes and Stellwagen [30, 33, 34], using both the geometric mean radius \bar{R} and the root-mean-square (rms) radius of gyration of a wormlike coil, R_G , to estimate DNA molecular size. The pore size values determined were strongly dependent on the parameters used for their estimation; when \bar{R} was used, the calculated gel pore radii decreased from ca. 5 nm to 0.6 nm when the gel concentration ranged from 3.5 to 10.5%T, 3.0%C, whereas larger values were found, from 30 to 3 nm, using R_G instead of \bar{R} to estimate DNA size. In the extended Ogston theory, the macromolecular size of a DNA fragment having a mobility corresponding to one-half of the mobility in free solution represents the average pore size of the corresponding gel. In the present work we evaluated the pore size according to [30] using \bar{R} to assess the DNA size; our data concerning the polyacrylamide are shown in Fig. 6 (line a). The



Figure 6. Log-log plots representing the dependence of the apparent gel pore size, R_p , as a function of polyacrylamide concentrations in (a) 3.3% Bis cross-linked acrylamide gels, (b) hybrid gels with 4.7% agarose as w/w of acrylamide, (c) hybrid gels with 10% agarose (w/w of acrylamide). R_p , geometric radius, was used for DNA size measurement. The slope values of the straight lines extrapolated by linear regression from the experimental values are: (a) -1.025 , (b) -1.1 , and (c) -0.63 .

apparent pore radius as a function of acrylamide concentration is represented in the log-log plot of Fig. 6: pore sizes from 3.2 nm (4%T, 3.3%C) to 1.2 nm (in 10%T, 3.3%C). These values sufficiently agreed with the determinations of [30]. The slope of the line is -1.1 ; the value is much larger than the value of -0.5 predicted by the extended Ogston theory. The double log graph of Fig. 6 (curve b) shows the dependency of the mixed-bed gel pore size on the percentage of polyacrylamide of the gels containing 4.7% of agarose over the acrylamide concentration. The curve has a slightly different slope of -1.05 and the size of the pores decreases from 4.64 to 1.39 nm when the concentration increases from 3 to 10% of polyacrylamide. The gels also have an optimal mechanical resistance at the lowest acrylamide concentrations. By increasing the amount of agarose (activated with double bonds and regular LE agarose) up to the optimal value of 10% over the polyacrylamide concentrations, easy-to-handle gels are obtained with concentrations of polyacrylamide as low as 1.5%. Their porosity is shown in Fig. 6 (curve c). The line has a slope of -0.63 , a value close to the theoretical value predicted by the Ogston extended theory. When the acrylamide concentration is 2%, the porosity of these gels reaches the value of 7.48 nm.

4 Discussion

In the literature there is no agreement on the data regarding the real size of polyacrylamide gels ([7] and references therein). However, different authors using different approaches have arrived at the same conclusions: (i) at any given %T the minimum pore radii are found in gels containing 5 or 10%C; (ii) the maximum pore radii are observed in gels containing a low %C (1–2%). The electrophoretic mobility of linear DNA, proportional to the gel porosity, is, in mixed-bed matrices, higher than the mobility observed in polyacrylamide gels of the same %T, analogously to that observed for low cross-linked gels when compared with 5%C cross-linked gels. The practical use of large porosity, low cross-linked polyacrylamide gels, in electrophoresis, is limited as a result



Figure 7. Log-log plot of absolute mobility versus DNA fragments size (in bp) in 1.2% agarose (curve a) run at 4 V/cm, hybrid gel (2%T, 10% w/w of acrylamide agarose (curve b) and 4%T, 3.3%C, polyacrylamide (curve c) both run at 10 V/cm.

of their poor mechanical strength. The mixed-bed gels, on the contrary, seem to have strong mechanical properties and are remarkably elastic also at low polyacrylamide concentrations.

Another important feature of this mixed-bed system is the ability to form handy gels also at low concentrations of polyacrylamide (1.5–2%) in the presence of at least 0.2% agarose, since agarose favors gelation during polymerization. DNA molecules exhibit an extremely high mobility in dilute gels. This is expected, since the absolute mobility of a given DNA fragment increases rapidly when enlarging the pore radius by decreasing %T at constant %C. Figure 7 shows the comparison between the mobility of the same DNA markers in three different matrices: LE agarose 1.2%, polyacrylamide 4%T, 3.3%C, and 2%T, 10% agarose mixed-bed gel. The absolute mobility observed in hybrid gels is close to that observed in a 1.2% agarose gel. Figure 8 shows the electrophoretic profile of the separation in the three different matrices. The resolution of fragments ranging from 60 to 500 bp is easily achieved in the two matrices containing polyacrylamide, whereas lower resolution is obtained in the agarose gels. Even though agarose is the matrix of choice for higher molecular mass fragments, from 2000 to 23000 bp, nevertheless hybrid gels seem to be porous enough to allow the penetration of these fragments. This new matrix appears to be able to extend the interval of molecular sizes that can be separated on a single gel, at the same time offering good resolution for small and large DNA fragments.

The apparent absolute mobility of DNA fragments in hybrid gels was compared with the mobility of the same fragments in polyacrylamide matrices, and Ferguson plots were employed to deduce pore size values of the two systems evaluated in the same conditions. The determination of the pore size of the two most widely used electrophoretic supports, polyacrylamide and agarose, has been the object of extensive investigations these past 10 years. One possible approach to this problem is to study the apparent absolute mobility of linear DNA fragments by constructing Ferguson plots. According to the extended Ogston theory of pore size distribution, the volume fraction $P(R_v)$ of pores in a random network of linear fibers, large enough to admit a sphere of radius R_v , is

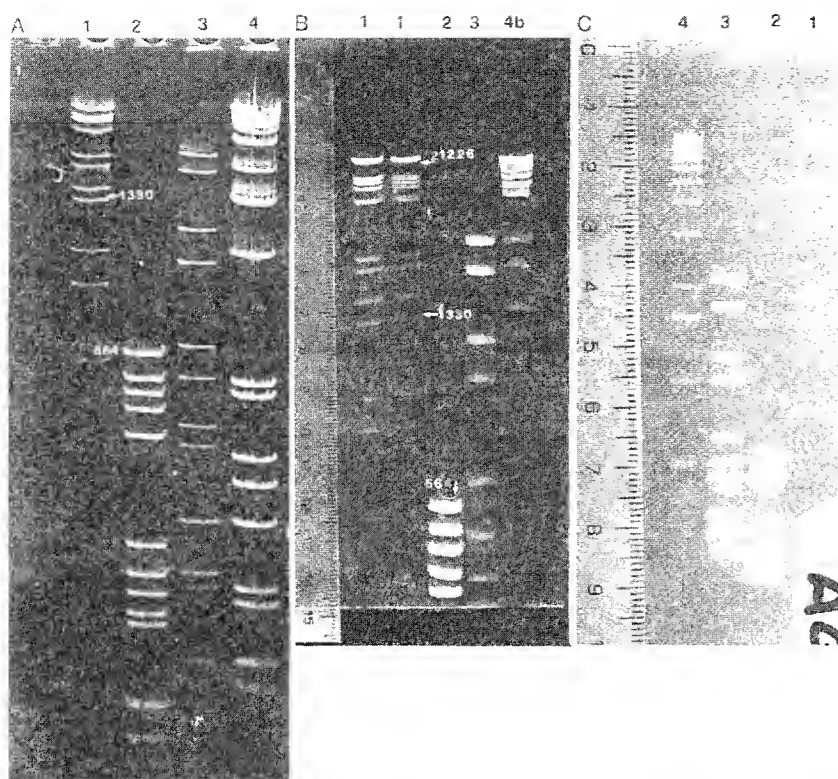


Figure 8. Separation of DNA fragments in (A) polyacrylamide 4%T, 3.3%C gel, (B) hybrid gel containing 2% acrylamide, 10% agarose (expressed as w/w of polyacrylamide), (C) 1.2% agarose. The conventional polyacrylamide gel was run at 10 V/cm for 200 min, the mixed-bed gel was run at 6.5 V/cm for 500 min, the agarose gel was run at 4 V/cm for 195 min. Samples: (1) marker III, (2) marker V, (3) marker VI, (4) and (4b) 1 kbp ladder.

$$P(R_M) = e^{-v(r+R_M)} \quad (3)$$

where v is the average number of fibers per unit volume, l is the average fiber length, and r is the fiber radius. Assuming that $vl \propto T$, where T is the gel concentration, and that the mobility μ of a DNA fragment of size R_M is proportional to the volume fraction of the gel it can enter, Eq. (3) leads to the relation

$$\log \mu = \log \mu_0 - K_R T \quad (4)$$

According to this model, $\log \mu$ vs. %T plots give straight lines, with slope K_R and intercept $\log \mu_0$. From Eq. (3) the average pore size a is calculated from the Ferguson plots by determining the gel concentration at which the mobility of a given DNA fragment is equal to one-half its mobility at zero gel concentration.

However, there are considerable limitations to the above model. In the extended Ogston theory DNA fragments are considered as rigid objects; in reality, the electric field produces a deformation on the DNA conformation, forcing the macromolecules to pass through pores which are too small for them. The effective radius R_M of the molecules itself is not unequivocally defined and the use of the mean geometric radius, R , instead of R_g , leads to an estimation of the pore size which differs by one order of magnitude. Moreover, the Ogston theory does not consider the way in which the pores, available to a particular fragment of size R_M , are connected; a large volume of unconnected pores is not used for migration. Given the above limitations, we do not aim at assessing abso-

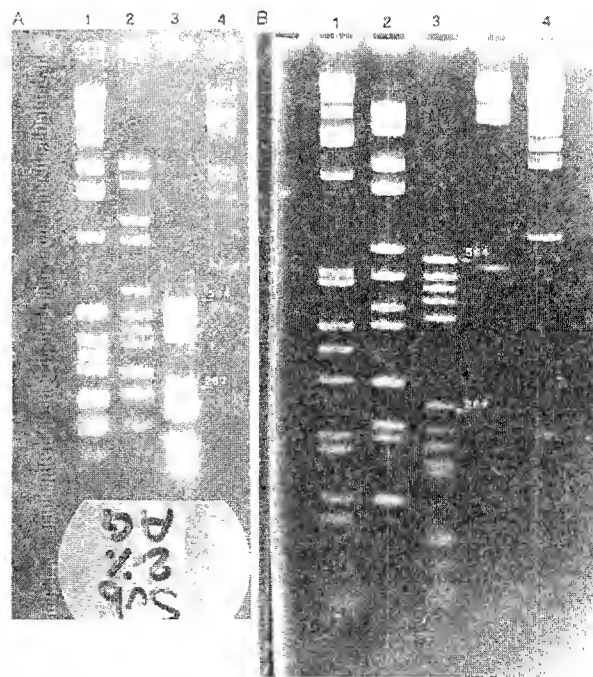


Figure 9. DNA molecular mass marker separation in (A) 2% agarose gel, (B) hybrid gel 2%T, 10% agarose (w/w% of acrylamide). Both gels are cast and run in a horizontal submarine system. The agarose gel was run at 4 V/cm in TAE buffer for 180 min, the hybrid gel was run at 6.5 V/cm for 240 min. Samples: (1) 1 kbp ladder, (2) marker VI, (3) marker V, and (4) marker III.

late pore size values for our new polymers using the Ogston model since we are conscious of the high number of variables involved in this determination. Therefore, to investigate the pore size differences between new and conventional polyacrylamide matrices, a comparative study was performed on the pore size determination of both systems. As previously discussed, we selected a method based on the use of Ferguson plots and employing the mean geometric radius, \bar{R} to assess the macromolecular DNA size value. The polyacrylamide pore size values that we found agree with the data previously calculated with the same method [30]. The results of the systematic study performed on our system leads to the following conclusions: (i) Ferguson plots of low molecular mass DNA fragments are almost parallel, and extrapolate to different mobilities at zero gel concentration; (ii) gels containing polyacrylamide, covalently linked to agarose, exhibit an average pore size value that is 30% higher than the value of a regular 3.3% Bis gel cross-linked with the same %T; (iii) increasing the agarose concentration (10% of the total amount of polyacrylamide), low-acrylamide containing gels (1.5–2%) are reproducibly obtained; their pores are 130% larger than the pores of a 4%T, 3.3%C polyacrylamide gel. In general, mixed-bed gels were found to be more elastic and mechanically stronger than classical polyacrylamide gels since an agarose-induced gelation process takes place during their polymerization. As a result of this latter event, the gels are not inhibited by atmospheric oxygen during their polymerization. Hybrid gels can be cast between glass and then run in a vertical system or polymerized at open face and then run horizontally as classical agarose gels. As shown in Fig. 9, this system provides an important tool for rapid and easy separations of low molecular mass fragments, i.e. PCR products, that can be analyzed in a system similar to a classical agarose horizontal gel yet offering the typical resolution of the more powerful polyacrylamide technique.

M. Chiari and P. G. Righetti are supported by grants from the European Community, Human Genome Project: GENE-CT 93-0024 and GENE-CT93-0018, respectively.

Received December 3, 1994

5 References

- [1] Chrambach, A. *The Practice of Quantitative Gel Electrophoresis*. VCH, Weinheim 1985, p. 64.
- [2] Norton, I. T., Goedali, D. M., Ansien, K. R. J., Morris, F. R., Ree, D. A., *Biopolymers* 1986, 25, 1009.
- [3] Boschetti, E., in: Dean, P. D. G., Johnson, W. S., Middle, I. (Eds.), *Affinity Chromatography*. IRI Press, Oxford 198, pp. 11–15.
- [4] Chiari, M., Micheletti, C., Nesi, M., Fazio, M., Righetti, P. G. *Electrophoresis* 1994, 15, 177–186.
- [5] Philipps, A. P., Baltzy, R., *J. Amer. Chem. Soc.* 1947, 69, 206–20.
- [6] Smith, C. L., Ewing, M., Mailon, M. T., Kane, S. F., Jain, T. Short, R. G., *J. Biochem. Biophys. Methods* 1989, 19, 51–64.
- [7] Righetti, P. G., Caglio, S., Saracchi, M., Quaroni, S., *Electrophoresis* 1992, 13, 581–595.
- [8] Weisich, E., De Bisi, P., Righetti, P. G., *Electrophoresis* 1993, 14, 583–590.
- [9] Fawcett, J. M., Morris, C. J. O. R., *Separ. Sci.* 1966, 1, 9–2.
- [10] Ornstein, L., *Ann. N. Y. Acad. Sci.* 1964, 121, 321–349.
- [11] Hendrick, J. L., Smith, A. J., *Arch. Biochem. Biophys.* 1968, 12, 155–162.
- [12] McDevitt, C. A., Muir, H., *Anal. Biochem.* 1971, 44, 612–62.
- [13] Peacock, A. C., Dingman, C. W., *Biochemistry* 1968, 7, 668–77.
- [14] Wolf, G., Casper, R., *J. Gen. Virol.* 1971, 12, 325–329.
- [15] Marcel, Y. L., Theolis, R. Jr., Milne, R. W., *J. Biol. Chem.* 198, 257, 13165–13168.
- [16] Moulin, S., Frechart, J. C., Dewailly, P., Szille, G., *Chim. Clin. Acta* 1979, 91, 159–163.
- [17] Lee, L. T., Lefevre, M., Wong, L., Roheim, P. S., Thompson, J., *Anal. Biochem.* 1987, 162, 420–426.
- [18] Horowitz, P. M., Lee, J. C., Williams, G. A., Williams, R. I., Barnes, L. D., *Anal. Biochem.* 1984, 143, 333–340.
- [19] Bode, H. J., in: Radola, B. J. (Ed.), *Electrophoresis '79*, Walter de Gruyter, Berlin 1980, pp. 39–46.
- [20] Tietz, D., Gottlieb, M. H., Fawcett, J. S., Chrambach, A., *Electrophoresis* 1986, 7, 217.
- [21] Chiari, M., Nesi, M., Righetti, P. G., *J. Chromatogr.* 1993, 65, 31–39.
- [22] Nechumson, S., *European Patent* 00879951B1.
- [23] Ogston, A. G., *Trans. Faraday Soc.* 1958, 54, 1754–1757.
- [24] Rodbard, D., Chrambach, A., *Proc. Natl. Acad. Sci. USA* 1970, 67, 970–977.
- [25] Ferguson, K. A., *Metabolism* 1964, 13, 985–1002.
- [26] Rodbard, D., in: Catsimpoolas, N. (Ed.), *Methods of Protein Separation*, Plenum, New York, 1976, Vol. 2, pp. 145–179.
- [27] Laurent, T. C., Killander, J., *J. Chromatogr.* 1964, 14, 317–33.
- [28] Stellwagen, N. C., *Biopolymers* 1985, 224, 2243–2255.
- [29] Slater, G. W., Noolandi, J., Turmel, C., Lalonde, M., *Biopolymers* 1968, 27, 509–524.
- [30] Holmes, D., Stellwagen, N. C., *Electrophoresis* 1991, 12, 253–26.
- [31] Stellwagen, N. C., *Biochemistry* 1983, 22, 6186–6193.
- [32] Japhe, W., Lahaye, M., *Carbohydr. Res.* 1989, 190, 249–265.
- [33] Holmes, D., Stellwagen, N. C., *Electrophoresis* 1990, 11, 649–65.
- [34] Holmes, D., Stellwagen, N. C., *Electrophoresis* 1991, 12, 612–61.
- [35] Olivera, B. M., Baine, P., Davidson, N., *Biopolymers* 1964, 245–257.
- [36] Chrambach, A., Rodbard, D., *Science* 1971, 170, 440–451.

EXHIBIT E

- [20] Serwer, P., Merrill, G., Moreno, E. T. and Hermann, R., *Prot. Biol. Fluids*, 1985, **33**, 517-520.
- [21] Holmes, D. L. and Stellwagen, N. C., *Electrophoresis* 1990, **11**, 5-14.
- [22] Olvera, B. M., Baine, P. and Davidson, M., *Biopolymers* 1964, **2**, 245-257.
- [23] Mathew, M. K., Smith, C. L. and Cantor, C. R., *Biochemistry* 1988, **27**, 9204-9210.
- [24] Serwer, P., *Anal. Biochem.* 1985, **144**, 172-178.
- [25] Orbán, L., Sullivan, J. V., Zwieb, C. and Chrambach, A., *Electrophoresis* 1989, **10**, 726-728.
- [26] Wieme, R. J., *Agar Gel Electrophoresis*, Elsevier, Amsterdam, 1965, pp. 68-77.
- [27] Jovin, T. M., Dante, M. L. and Chrambach, A., *Multiphasic Buffer Systems Output*, National Technical Information Service, Springfield, VI, 1970, PB 196085 to 196091, 259309 to 259312, 203016.
- [28] Orbán, L. and Chrambach, A., *Electrophoresis* 1991, **12**, 241-246.
- [29] Orbán, L., Fawcett, J. S., Sullivan, J. V., Chidake, B. J. and Chrambach, A., *Electrophoresis* 1988, **9**, 32-36.

Diana L. Holmes
Nancy C. Stellwagen

Department of Biochemistry
University of Iowa
Iowa City, IA

Estimation of polyacrylamide gel pore size from Ferguson plots of normal and anomalously migrating DNA fragments

I. Gels containing 3 % N,N'-methylenebisacrylamide

The mobilities of normal and anomalously migrating DNA fragments were determined in polyacrylamide gels of different acrylamide concentrations, polymerized with 3 % N,N'-methylenebisacrylamide as the crosslinker. The DNA samples were a commercially available 123-bp ladder and two molecular weight ladders containing multiple copies of two 147-base pair (bp) restriction fragments, obtained from the *MspI* digestion of plasmid pBR322. One of the 147 bp fragments is known to migrate anomalously slowly in polyacrylamide gels. Ferguson plots were constructed for all multimer ladders, using both absolute mobilities and relative mobilities with respect to the smallest DNA molecule in each data set. If the retardation coefficients were calculated from the relative mobilities, and the rms radius of gyration was used as the measure of DNA size, the Ogston equations were obeyed and the gel fiber parameters could be calculated. The effective pore sizes of the gels were estimated from the gel concentration at which the mobility of a given DNA molecule was reduced to one-half its mobility at zero gel concentration. The estimated pore radii ranged from ~130 nm for 3.5 % gels to ~70 nm for 10.5 % gels. These values are much larger than the pore sizes previously determined for the polyacrylamide matrix.

1 Introduction

Certain double-stranded DNA fragments exhibit anomalous mobilities in polyacrylamide gels (reviews: [1-4]). The mobilities of the anomalously migrating fragments are either slower [5-8] or faster [5, 9] than expected on the basis of their known molecular weights. Anomalously slowly migrating fragments often contain runs of adenine (A) or thymine (T) residues in

phase with the helix repeat [7, 10, 11], although some anomalously slowly migrating guanine-cytosine (G-C) rich fragments are also known [8, 9, 12, 13]. Many of the anomalously slowly migrating fragments appear to be stably curved or bent; such fragments exhibit curvature when visualized in the electron microscope [14, 15], have enhanced rates of ligase-catalyzed circle formation [16, 17], and/or exhibit electric birefringence or dichroism relaxation times that are faster than observed for normally migrating fragments of the same molecular weight. Faster relaxation times are consistent with curvature of the anomalously migrating fragments [18-20].

Why curved DNA fragments exhibit anomalously slow electrophoretic mobilities in polyacrylamide gels is not well understood. The mobility anomaly increases with increasing polyacrylamide concentration [7, 8, 21-23], suggesting that the curved molecules require larger pores through which to migrate [7, 22, 24-26]. Correlations have been made between the extent of the mobility anomaly and the degree of curvature of the DNA fragments [25-27]. However, a recent study has

Correspondence: Dr. Nancy C. Stellwagen, Department of Biochemistry, University of Iowa, Iowa City, Iowa 52242 USA

Abbreviations: Bis, N,N'-methylenebisacrylamide; bp, base pairs; BSA, bovine serum albumin; C, crosslinker concentration; EDTA, ethylenediaminetetraacetic acid; K_R , retardation coefficient; L, contour length; $\mu_{0.0}$, absolute mobility; μ_{rel} , relative mobility; p, persistence length; \bar{R} , geometric mean radius; R_g , rms radius of gyration; rms, root-mean-square; T, total concentration of acrylamide and Bis; TAE, Tris-acetate buffer; TBE, Tris-borate buffer; TEMED, N,N,N',N'-tetramethylethylenediamine; Tris, tris (hydroxymethyl) aminomethane.

suggested that pore size alone cannot be responsible for the anomalous mobility of curved DNA fragments in polyacrylamide gels, because increasing the pore size does not eliminate the anomalous mobility [23]. In addition, anomalous mobilities are not observed for curved fragments in agarose gels ranging up to 9 % in concentration [2, 8, 9, 21, 23].

The pore sizes used in the previous study [23] to evaluate the anomalous mobility of fragment 12A and its multimers in polyacrylamide gels were taken from values in the literature. These pore sizes were determined from the mobility of proteins [28-30] or small DNA restriction fragments [8] in polyacrylamide gels, using the extended Ogston theory of pore size distribution to estimate pore size ([30-32], reviews: [2, 33, 34]). However, pore sizes have been determined for only a limited number of acrylamide and crosslinker concentrations. In addition, the pore sizes determined in the various studies agree with each other only in order of magnitude [23]. Therefore, in the present work we have made an extensive and systematic study of the mobility of various DNA fragments in polyacrylamide gels of various compositions, in order to determine a consistent set of effective pore sizes in the various gels.

In the first paper in this series, mobilities were measured for normal and anomalously migrating DNA fragments in polyacrylamide gels containing 3 % *N*, *N'*-methylenebisacrylamide (Bis) as crosslinker. Ferguson plots (logarithm of mobility vs. gel concentration [35]) were constructed using both absolute mobilities and relative mobilities with respect to the smallest DNA molecule in each molecular weight ladder. Retardation coefficients were calculated for the various DNA fragments from the two types of Ferguson plots, using two different methods to estimate DNA size. The results suggest that the Ogston equations are obeyed and gel fiber parameters can be estimated if the Ferguson plots are constructed from relative mobilities and the size of the DNA molecules is estimated from the root-mean-square (rms) radius of gyration. In the second paper of this series, the pore sizes of a variety of polyacrylamide gels of different crosslinker concentrations will be compared. The third paper in this series will present an analysis of the effect of gel pore size on the anomalous mobility of the curved DNA fragment studied here. The final paper in this series will present an analysis of the retardation coefficients obtained for different fragments in gels of different crosslinker concentrations.

2 Materials and methods

2.1 Materials

2.1.1 DNA ladders

Three different DNA molecular weight "ladders" were used for the studies reported here. Each of the ladders consists of a series of DNA molecules containing different numbers of monomer fragments. (The term "ladder" comes from the relatively even spacing of such multimers on an electrophoresis gel.) Two of the monomers were the two 147-bp fragments, called 12A and 12B, obtained from the *Msp*I digestion of plasmid pBR322 [36]. Fragment 12B migrates normally in polyacrylamide gels, but fragment 12A migrates anomalously slowly [8, 21, 23]. Because of cloning procedures, each monomer in these two multimer ladders contains 167 base pairs, plus four unpaired bases at each end. The cloning procedures

and methods used to generate the molecular weight ladders have been described in detail previously [23, 37]. The third molecular weight ladder used for the present studies was a commercially available 123 bp ladder (Cat. No. 56135A, Bethesda Research Laboratories, Gaithersburg, MD). The DNA molecules in this ladder migrate normally in polyacrylamide gels [23].

2.1.2 Gel media

Acrylamide and Bis were Ultrapure Electrophoresis Grade reagents purchased from Bethesda Research Laboratories. *N,N,N',N'*-Tetramethylethylenediamine (TEMED) was purchased from Fisher Scientific (Fair Lawn, NJ). Ethidium bromide was purchased from Sigma (St. Louis, MO). All other chemicals were reagent grade.

2.2 Methods

2.2.1 Preparation of polyacrylamide gels

For all experiments reported here, 15.5 × 26.5 × 0.15 cm slab gels were used, cast between glass plates as described [38]. The gels were supported in a home built gel cabinet similar to those available commercially. A detailed description of the gel apparatus and the methods used to prepare the gels will be presented separately. Briefly, the desired quantities of acrylamide and Bis were dissolved separately in distilled water, mixed and diluted to the proper concentration with TBE buffer (TBE: 0.032 M boric acid, 0.05 M Tris base, and 1 mM EDTA, pH 8.2). Then 0.1 % w/v freshly dissolved ammonium persulfate and 0.1 % v/v TEMED were added, and the solutions were mixed and quickly poured into the previously prepared gel form. Gelation usually occurred within 5-15 min, depending on the acrylamide concentration. Each gel was aged overnight in a gel cabinet containing TBE, in order to allow the polymerization reaction to proceed to completion [39]. The polyacrylamide concentration in each gel (%T) is given as the total w/v concentration of acrylamide plus Bis. The crosslinker concentration (%C) is given as the w/w percentage of Bis included in %T; for the studies reported here, the Bis concentration was always 3 %.

2.2.2 Electrophoresis

Electrophoresis was carried out in a vertical slab gel apparatus of standard design [8, 38]. The electric field was supplied by a HeathKit Model SP 2717A regulated power supply (Benton Harbor, MI). The applied voltage was always 100 V, corresponding to an effective field strength in the gel of 3.3 V/cm (from the applied voltage and the distance between the electrodes). The actual voltage in the gel was measured to be 3.3 V/cm in a separate experiment, using a Fluke digital multimeter, Model 75 (Everett, WA). Control experiments indicated that the variation of the effective field strength from one experiment to another was about ± 2 %. All gels were run at room temperature, 23° C. The temperature was constant across the length and breadth of the gels, as measured by a digital liquid crystal thermometer strip (Sargent-Welch, Skokie, IL) attached to the outer gel plate. The uniformity of temperature across the width of the gel was also indicated by the absence of "smiling" effects. All gels were pre-electrophoresed at 3.3 V/cm for at least 2 h before the samples were

loaded, to remove polar impurities [8]. The DNA samples typically contained about 1 μ g of a DNA ladder diluted to 8.0 μ L with T0.1E buffer (10 mM Tris-HCl buffer, pH 8.0, plus 0.1 mM EDTA); each solution also contained 0.8 μ L of a solution containing 1 μ g/ μ L Bromophenol Blue marker dye in 50 % glycerol. After preparation, the DNA solutions were vortexed and layered under the buffer in the 9 \times 1.5 mm wells of the gel. Each gel also included a lane with one of the plasmids digested to completion, to mark the position of the monomer band. Complete digests contained only the 12A or 12B monomer fragment and two fragments of the vector (1427 and 2936 bp). All gels were run at $E = 3.3$ V/cm, a field strength at which the mobilities are independent of E [23]. The duration of electrophoresis ranged from 4 to 40 h, depending on the composition of the gel; all gels were run until the monomer bands had migrated 50–90 % of the length of the gel. After electrophoresis, the gels were stained 15 min in a solution containing 2.5 μ g/L ethidium bromide. Mobilities were determined from photographs of the stained gels, using a Polaroid MP 4 Land camera and Polaroid Type 57 high speed film with a No. 23a wrattan filter. All measurements of migration distances were made from the photographs, using the measurement of a ruler photographed simultaneously to provide the magnification factor. A photograph of a typical electrophoresis gel is shown in Fig. 1.

2.2.3 Calculation of absolute and relative mobilities

The apparent absolute mobilities of the DNA fragments in the various gels were calculated from Eq. (1).

$$\mu_{abs} = \frac{d}{E t} \quad (1)$$

where μ_{abs} is the absolute mobility, d is the distance in cm migrated by a given fragment in the gel, E is the electric field strength in V/cm, and t is the time in seconds. The absolute mobilities calculated for the various DNA fragments in different independently prepared gels of identical composition agreed within ± 5 %. Relative mobilities, μ_{rel} , were calculated for each of the DNA fragments in each of the molecular weight ladders using the mobility of the monomer of each individual multimer ladder as the reference mobility, according to Eq. (2).

$$\mu_{rel} = \frac{(\mu_{abs})_n}{(\mu_{abs})_1} \quad (2)$$

where $(\mu_{abs})_n$ is the absolute mobility of the dimer to n -mer and $(\mu_{abs})_1$ is the absolute mobility of the smallest molecule in the data set. For consistency, the reference mobility was chosen to be the mobility of the monomer of the molecular weight ladder being characterized.

2.2.4 Calculation of Ferguson plots

Ferguson plots [35] were constructed for each of the DNA fragments in each of the molecular weight ladders by plotting the logarithm of the absolute mobility of the fragment as a function of gel concentration, %T. The negative slope of such a plot is defined as the retardation coefficient, K_R , using the relation:

$$\ln \mu = \ln \mu_0 - K_R T \quad (3)$$

where $\ln \mu$ is the natural logarithm of the observed mobility and μ_0 is the mobility extrapolated to zero gel concentration. Note

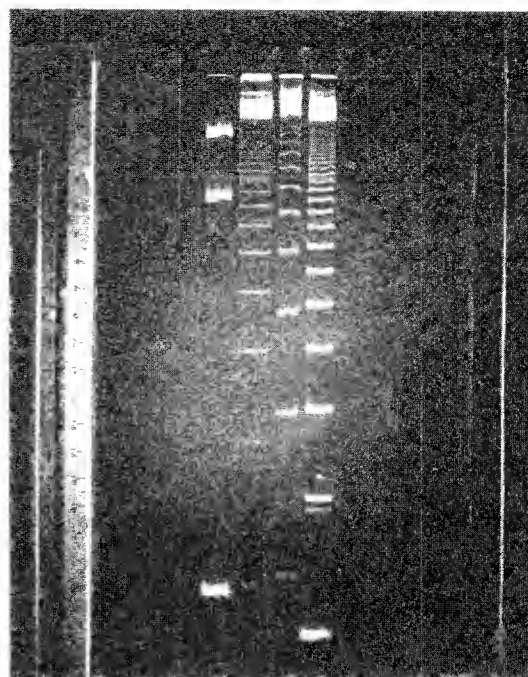


Figure 1. Photograph of a typical polyacrylamide gel, 5.7 %T, 3 %C, cast and run in TBE buffer. From left to right the lanes contain: lane (1) plasmid PB20 digested to completion with *Eco*RI (molecular weights 2936, 1427 and 153 bp from top to bottom); (2) the 12B multimer ladder (multiples of 167 bp); (3) the 12A multimer ladder (multiples of 167 bp; these fragments migrate more slowly than the corresponding 12B multimers); (4) the 123 bp ladder.

that this definition of K_R differs from others in the literature based on $\log_{10} \mu$ [32–34]. As discussed previously [40], it is not clear that absolute mobilities are appropriate for analyzing data using the extended Ogston theory. The Ogston equations do not take into account a variety of factors which might influence the absolute mobility, such as interactions of the DNA molecules with the matrix [23, 36] and/or the effect of different buffer ions on the observed mobility (D. L. Holmes and N. C. Stellwagen, in preparation). To interpret differences in mobility between molecules that differ only in molecular weight, it would seem logical to analyze the data in terms of relative mobilities, calculated with respect to the mobility of the smallest DNA molecule in the data set. Therefore, Ferguson plots were also constructed for each of the DNA fragments using relative mobilities calculated from Eq. (2), and the corresponding retardation coefficients were determined. A similar analysis has recently been applied to the electrophoresis of DNA in agarose gels [40]. The retardation coefficients calculated from Ferguson plots based on relative mobilities are different from the retardation coefficients calculated from Ferguson plots based on absolute mobilities, since the mobility of the reference DNA is dependent on gel concentration (compare Figs. 4 and 9, below). Only if the mobility of the reference were independent of gel concentration would the retardation coefficients obtained from the Ferguson plots of absolute and relative mobilities be identical. In the past, Ferguson plots have often been constructed as plots of relative mobility vs. gel concentration, using the mobility of a marker dye or of the moving boundary in a discontinuous buffer system as the reference mobility [8, 34]. However, it has been

found that the mobilities of the moving boundary [41] and the commonly used reference dye Bromophenol Blue [8, 42] depend on the polyacrylamide gel concentration. Hence, most Ferguson plots constructed in the past have also been based on references whose mobilities were dependent on gel concentration. Therefore, using the mobility of a low molecular weight DNA molecule as the reference mobility in the present work differs only in degree from traditional procedures [40].*

2.2.5 Estimation of gel pore size from Ferguson plots

According to the Ogston theory of pore size distribution [31], extended by Rodbard and Chrambach [30, 32, 33], the retardation of macromolecules during gel electrophoresis is assumed to be related to the fractional volume of spaces in the matrix available to the migrating macromolecule. Therefore, Ferguson plots can be used to estimate the effective pore size of polyacrylamide gels by determining the gel concentration at which the mobility of a given DNA fragment is equal to one-half its mobility at zero gel concentration. At this gel concentration, assuming a Gaussian distribution of pore sizes, a macromolecule with a size equal to the median pore radius of the gel should just be able to access half the available volume in the gel. Therefore, at this gel concentration the radius of the migrating macromolecule should be equal to the median pore radius of the gel [29, 32, 33, 44-46]. To calculate the effective pore radius of the polyacrylamide matrix, the Ferguson plots of each DNA fragment in each gel were extrapolated to zero gel concentration by linear regression, assuming the slopes of the lines to remain constant at very low gel concentrations (see the discussion of this point below). The gel concentration at which $\mu = \mu_0/2$ (μ : mobility; μ_0 : mobility at zero gel concentration) was determined for each DNA fragment in each gel. The relationship between the median pore radius and gel concentration was then determined from a double logarithmic plot of apparent pore radius as a function of gel concentration. Since the extended Ogston theory assumes that the gel pore radii have an asymmetric Poisson distribution [30-34], the median pore radius determined by the Ferguson plot method is different from the mean pore radius determined by standard methods based on the extended Ogston theory [31, 32, 34]. However, the two methods should give similar results, since Fawcett and Morris [29] found that median and mean pore radii differed only by about 10 % in polyacrylamide gels of a variety of compositions.

2.2.6 Estimation of gel fiber parameters from retardation coefficients

According to the extended Ogston theory of pore size distribution, the retardation coefficients calculated from the Ferguson plots can be related to gel fiber parameters if some assumptions can be made about gel structure [32, 34]. If the gel is

assumed to be a "2-D" gel, characterized by an array of random planes, the retardation coefficients, K_R , are found to be proportional to the radii of the migrating macromolecules, R , according to Eq. (4):

$$K_R = k R \quad (4)$$

where k is a proportionality constant related to the surface area of the planes per unit volume of matrix [32, 47]. If the gel is assumed to be a "1-D" gel, i.e., composed primarily of fibers much longer than the radii of the migrating macromolecules, the retardation coefficients are proportional to the square of the macromolecular radius, according to Eq. (5):

$$K_R = \pi l' (r + R)^2 \quad (5)$$

where r is the effective gel fiber radius and l' is the total fiber length per gram of matrix. The negative intercept of R at $K_R^{-1/2} = 0$ is equal to the gel fiber radius; the slope of the line and the value of K_R at $r = -R$ can be used to calculate the total fiber length per gram of matrix [32-34]. For "0-D" gels containing very short fibers, the retardation coefficients are proportional to R^3 [32]. Other theoretical treatments of gel electrophoresis have deduced different relationships between restricted migration and macromolecular radius. Ogston [48] postulated a linear relationship between K_R and R in order to explain the retardation of the sedimentation and diffusion of compact macromolecules in solutions containing high molecular weight linear polymers. However, the retardation coefficients were determined from semilogarithmic plots of relative retardation vs. the square root of polymer concentration (in contrast to the Ferguson plots, which are semilogarithmic plots of mobility vs. the first power of gel concentration). Cobbs [49], analyzing gels as networks of parallel planes containing projections of the gel fibers, interpreted the retardation coefficients as:

$$K_R = c_i (R + r)^i \quad (6)$$

where the c_i are constants for any particular molecule and gel system and $i = 1, 2, 3, \dots$. Because of uncertainty as to the correct representation of the retardation coefficients in terms of macromolecular radius, the retardation coefficients obtained from the Ferguson plots in this study were plotted both as $K_R^{1/2}$ vs. R and K_R vs. R . Gel fiber parameters were estimated from plots of $K_R^{1/2}$ vs. R .

2.2.7 Evaluation of DNA macromolecular radius

In order to estimate the gel pore radius, or calculate the gel fiber parameters from Eq. (5), the radius of the migrating macromolecules must be known. For proteins, which are generally globular and approximately spherical in shape, the effective molecular radius has often been chosen to be the radius of a sphere of equal volume, which is a measurement based on $M^{1/3}$ [33]. For linear DNA molecules, which are highly asymmetric in shape, the most appropriate value to use for the molecular radius is not clear. In the past, both the geometric mean radius, i.e., the radius of a sphere equal in volume to the volume of the cylindrical DNA molecule [8, 50] and the root-mean-square (rms) radius of gyration [2, 45, 46, 50] were used to estimate DNA macromolecular size. For DNA the geometric mean radius \bar{R} , in nm, is defined [8, 50] as:

$$\bar{R} = 0.755 (\text{bp})^{1/3} \quad (6)$$

* The mobility of the moving boundary in polyacrylamide gels with 5 %C decreased by about 30 % when the polyacrylamide concentration was increased from 5 to 15 %T [41], a gel concentration range commonly used to determine the Ferguson plots of proteins [29, 43]. The mobility of the 12B monomer, used as one of the reference fragments in this study, decreased about fourfold when the gel concentration was increased from 3.5 to 10.5 %T. Although this decrease in mobility is much larger than observed for reference dyes [8, 42] and/or the moving boundary [41], the principle is the same. The mobility of the reference is not independent of gel concentration.

where bp is the number of base pairs in the fragment. The rms radius of gyration of a wormlike coil, R_G , is defined [51] as:

$$R_G = \alpha R_p^2 \approx l^2 = \left(\frac{pL}{3} \left[1 - \frac{p}{L} + \frac{p}{L} \exp(-L/p) \right] \right)^{1/2} \quad (7)$$

where L is the contour length of the fragment ($0.34 \text{ nm} \times \text{bp}$), and p is the persistence length, here taken of be 50 nm, an average value observed for DNA in solutions of moderate ionic strength [52-54].*

3 Results and discussion

3.1 Dependence of absolute mobility on DNA molecular weight

Typical plots of the logarithm of DNA molecular weight as a function of the observed mobility are shown in Fig. 2 for three representative gel concentrations. The sigmoidal shapes of these curves are clearly apparent. The mobilities of the 123-bp and 12B multimer ladders can be described by a common curve at all gel concentrations, indicating that the DNA molecules in both ladders migrate with mobilities appropriate for their respective molecular weights. The mobilities of fragment 12A and its multimers are smaller than the mobilities of other fragments of the same molecular weight. Therefore, the mobilities of fragment 12A and its multimers are described as anomalously slow.

The functional dependence of the mobility on DNA molecular weight can be seen more easily from log-log plots, as shown in

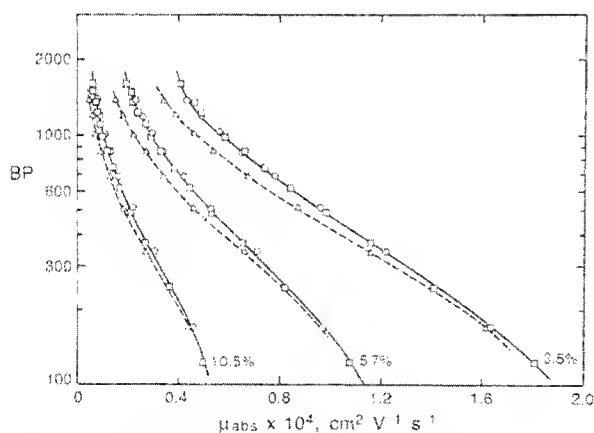


Figure 2. Semilogarithmic plots of molecular weight, in bp, as a function of absolute mobility for gels containing 3.5% (right), 5.7% (center) or 10.5% polyacrylamide (left curve). □, 123 bp ladder; ○, 12B multimer ladder; △, 12A multimer ladder.

* The flexibility of the DNA double helix is usually described by the wormlike chain model of Kratky and Porod [55]. In this model the DNA molecule is characterized by two parameters, its contour length, L , and a parameter that increases with increasing chain stiffness, the persistence length, p . The persistence length may be defined as the average sum of the projections of all the bonds of the chain onto the first one, i.e., the distance over which the directions of individual segment elements are correlated [52]. DNA persistence lengths have been determined by light scattering [53, 54, 56], flow birefringence [57], electric birefringence [58, 59], electron microscopy [60], and ligase-catalyzed cyclization of DNA [61].

Fig. 3. In this figure the mobilities measured in the current study are combined with the results of an earlier study [8], recalculated in terms of absolute mobilities, in order to illustrate a wider range of molecular weights. At high molecular weights, the mobilities of the various fragments decreased approximately inversely with molecular weight, as predicted by reptation theory [62-65]. At low molecular weights, the mobilities decreased approximately as $M^{-1/2}$. The slopes at both ends of the plot increased gradually in absolute value with increasing gel concentration (not shown), becoming -1.3 at high molecular weights and -0.40 at low molecular weights in gels containing 9.3 %T.

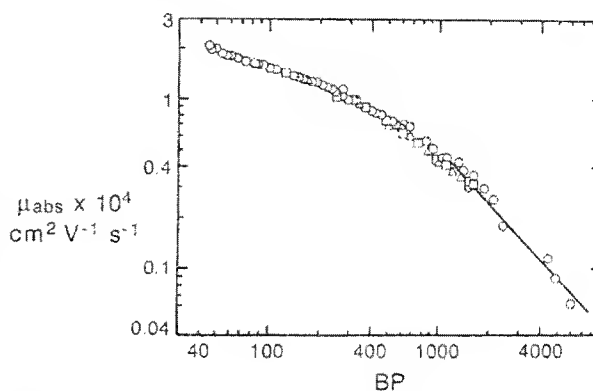


Figure 3. Log-log plot of absolute mobility as a function of DNA molecular weight, in bp, in gels containing 4.6% polyacrylamide. □, 123-bp ladder; △, 12B multimer ladder; ○, data from [8], recalculated in terms of absolute mobility. The slope of the drawn line at high molecular weights is -1.1 ; at low molecular weights the drawn line has a slope of -0.33 .

3.2 Ferguson plots constructed from absolute mobilities

Ferguson plots were constructed for each of the DNA fragments in each of the three multimer ladders using the apparent absolute mobilities observed in each of the polyacrylamide gels. Typical results are shown in Fig. 4 for the three multimer ladders. In all cases the Ferguson plots appeared to be linear over the range of polyacrylamide gel concentrations investigated, making the extrapolation to zero gel concentration unambiguous if it can be assumed that the curves remain linear in the concentration region where polyacrylamide does not form a gel. For the sake of simplicity, this assumption has been made in the studies reported here. The validity of this assumption is discussed in the next section. The straight lines in the Ferguson plots are nearly parallel and do not extrapolate to a common intercept at zero gel concentration, as predicted by the extended Ogston theory [30-34]. Therefore, the mobilities of the various DNA fragments at zero gel concentration (Y_0 values in the terminology of Rodbard and Chrambach [30, 32-34]) decrease markedly with increasing DNA molecular weight. Similar results have been reported previously for double-stranded nucleic acids in polyacrylamide gels [8, 66].

3.3 Mobility of DNA at zero gel concentration

The mobilities of the various DNA fragments, extrapolated to zero gel concentration, appear to converge to a limiting value of $3.8 \times 10^{-4} \text{ cm}^2 \text{ V}^{-1} \text{ s}^{-1}$ at low molecular weights, as shown in

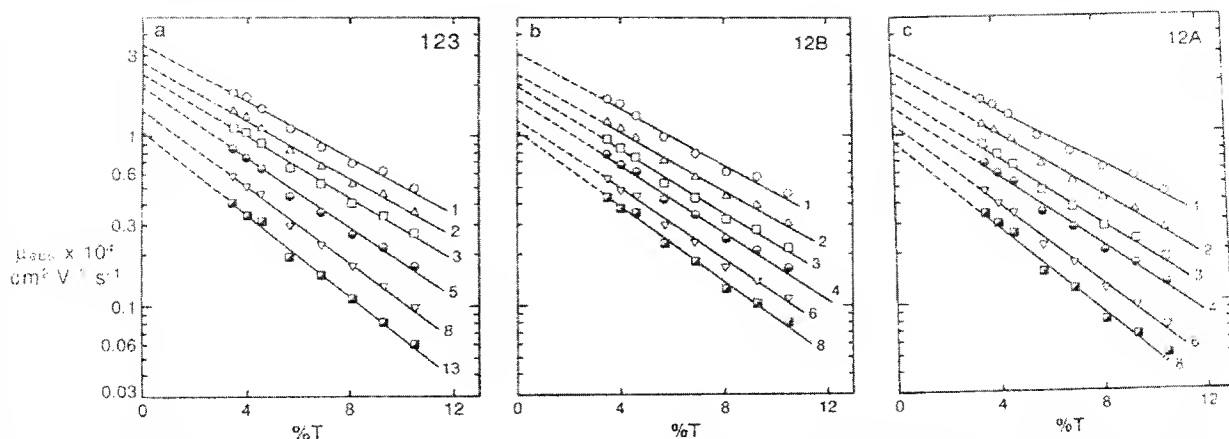


Figure 4. Ferguson plots based on absolute mobility. The logarithm of the absolute mobility, μ_{abs} , is plotted as a function of the polyacrylamide gel concentration, %T. The number of monomers in each multimer is indicated beside each curve. The extrapolations to zero gel concentration are indicated by dashed lines. More precise values of the slopes and intercepts were determined by linear regression.

Fig. 5. This figure includes data from the present study as well as the extensive data on low molecular weight fragments obtained in an earlier study [8]. The limiting mobility at low molecular weights can be compared with the mobility of DNA in free solution, which was measured to be $1.5\text{--}2.2 \times 10^{-4} \text{ cm}^2 \text{ V}^{-1} \text{ s}^{-1}$, depending on buffer concentration, at 1°C [67-69]. The free solution mobility is independent of molecular weight [67]. Taking a value of $2.0 \times 10^{-4} \text{ cm}^2 \text{ V}^{-1} \text{ s}^{-1}$ to be appropriate for the TBE buffers used in the present study, and converting the mobility to 23°C by multiplying by the ratio of the viscosity of water at the two temperatures [70], the mobility of DNA in free solution at 23°C is estimated to be $3.7 \times 10^{-4} \text{ cm}^2 \text{ V}^{-1} \text{ s}^{-1}$. This value is close to the experimental value of $3.8 \times 10^{-4} \text{ cm}^2 \text{ V}^{-1} \text{ s}^{-1}$, suggesting that the mobility observed for very small DNA fragments in the limit of zero polyacrylamide gel concentration is equal to the free solution mobility. This result also suggests that the linear extrapolation of the Ferguson plots to zero gel concentration is valid. The lower mobilities observed at zero gel concentration for the larger DNA fragments may be due to interactions of the larger fragments with the matrix, although curvature of the Ferguson plots of these fragments in the region of very low %T cannot be ruled out. The limiting mobility observed for small DNA fragments in polyacrylamide gels is much higher than the limiting mobility of $2.7 \times 10^{-4} \text{ cm}^2 \text{ V}^{-1} \text{ s}^{-1}$ observed in agarose gels [40, 50, and references therein], possibly because of the electroendosmosis of agarose [71]. Alternatively, the mobility ex-

trapolated to zero agarose gel concentration may be low because the DNA samples used in that study [40, 50] were much larger than the DNA fragments used in the present study.

3.4 Gel pore radius calculated from absolute mobilities

The pore sizes of polyacrylamide gels containing 3 % Bis were estimated from the Ferguson plots in Fig. 4, as described in Section 2.2.5, using both \bar{R} and R_G to estimate DNA molecular size. Log-log plots of the apparent pore radius as a function of gel concentration are given in Fig. 6 for the three multimer ladders. When \bar{R} was used to measure DNA size, the calculated gel pore radii decreased from ca. 5 nm to 0.6 nm when the gel concentration increased from 3.5 to 10.5 %T, as shown in Fig. 6a. These pore radii are close to the values previously

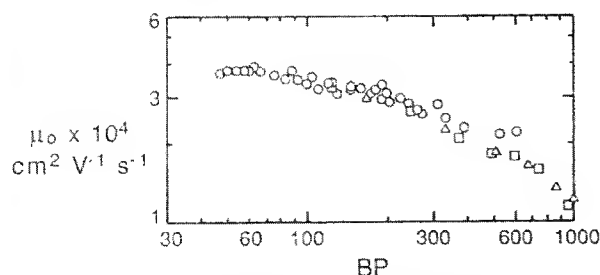


Figure 5. Log-log plot of the absolute mobility extrapolated to zero gel concentration, μ_0 , as a function of the number of base pairs (bp) in the fragment. \circ , data from [8], recalculated in terms of absolute mobilities; Δ , 12B multimer ladder; \square , 123 bp ladder.

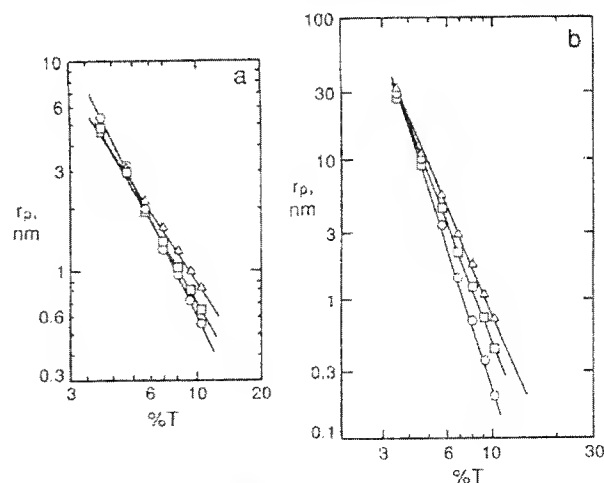


Figure 6. Log-log plots of the dependence of the apparent gel pore size, r_p , on polyacrylamide concentration, %T. The values of %T were determined from Ferguson plots based on absolute mobilities. (a) \bar{R} was used as the measure of DNA size; (b) R_G was used. The slopes of the straight lines were determined by linear regression. The slopes in (a) ranged from -1.6 to -2.0 for the three molecular weight ladders; in (b), the slopes ranged from -3.3 to -4.6. \square , 123-bp ladder; \circ , 12B multimer ladder; Δ , 12A multimer ladder.

determined from a study of small DNA restriction fragments in polyacrylamide gels [8]. Using R_G instead of \bar{R} to measure DNA size, the pore radii ranged from *ca.* 30 nm to *ca.* 0.3 nm as the gel concentration increased from 3.5 to 10.5 %T, as shown in Fig. 6b. In both cases, the exact value of the pore radius depended somewhat on the particular DNA molecular weight ladder used for the measurements. Surprisingly, this was true even for the 123-bp and 12B multimer ladders, whose mobilities were described by common curves in Fig. 2. The pore radii determined using the 12A multimer ladder are generally larger than the values determined using the other two molecular weight ladders, especially in gels containing ≥ 6 %T. This result is surprising, since one might have expected anomalously slowly migrating fragments to "see" a gel with effective pore sizes smaller than the pore sizes determined with normally migrating DNA fragments.

The slopes of the lines in Fig. 6a ranged from -1.6 for the anomalously migrating 12A multimer ladder to -2.0 for the normal 12B multimer ladder. The slopes of the lines in Fig. 6b ranged from -3.3 to -4.6 for the same two molecular weight ladders. These slopes are much larger than the value of -0.5 predicted by the extended Ogston theory [32].

3.5 Retardation coefficients based on absolute mobilities

To estimate gel fiber parameters, the square roots of the retardation coefficients calculated from the slopes of the Ferguson

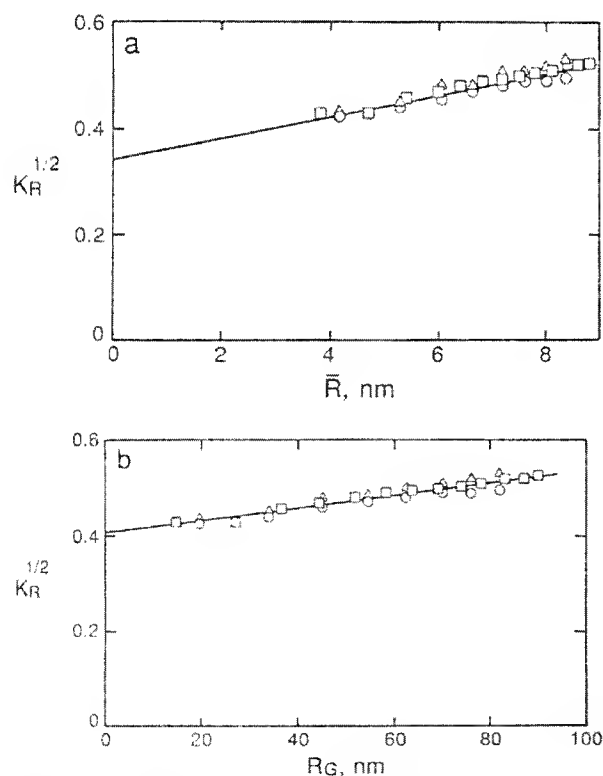


Figure 7. Plots of the square root of the retardation coefficient, $K_R^{1/2}$, as a function of molecular radius. (a) \bar{R} was used as the measure of DNA size; (b) R_G was used. The retardation coefficients were calculated from Ferguson plots based on absolute mobilities. \square , 123-bp ladder; \circ , 12B multimer ladder; Δ , 12A multimer ladder.

plots based on absolute mobilities (Fig. 4), were plotted as functions of \bar{R} or R_G , as shown in Figs. 7a and 7b, respectively. In each plot the data could be described by a single straight line, the slope of which was only weakly dependent on DNA molecular size. The apparent fiber radius (the negative intercept of \bar{R} or R_G at $K_R^{1/2} = 0$) was estimated to be ~ 18 nm from Fig. 7a and ~ 290 nm from Fig. 7b. Log log plots of the retardation coefficients as a function of \bar{R} or R_G (not shown) indicated that K_R increased approximately as the 0.5 power of \bar{R} or the 0.3 power of R_G , not as the square of molecular radius predicted by Eq. (5). This much weaker dependence of K_R on \bar{R} or R_G is the reason for the nearly horizontal slopes of the lines in Figs. 7a and 7b. The double logarithmic plot suggested that a plot of K_R vs. $\bar{R}^{1/2}$ should be linear; such a plot is shown in Fig. 8. Within experimental error, the data for the different molecular weight ladders can be described by straight lines. The intercepts at $K_R = 0$ occur at positive values of $\bar{R}^{1/2}$ for the 123-bp and 12A multimer ladders and negative values of $\bar{R}^{1/2}$ for the 12B multimer ladder. It is not possible to interpret these values because no theory describes the dependence of K_R on $\bar{R}^{1/2}$, however, it seems unlikely that both positive and negative intercepts can be rationalized. Similar plots of K_R vs. $R_G^{1/2}$ (not shown) were also linear; however, in this case all the intercepts of the straight lines with the abscissa at $K_R = 0$ were negative.

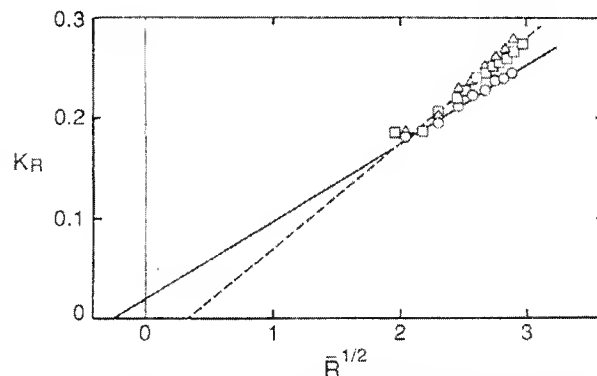


Figure 8. Dependence of the retardation coefficients based on absolute mobilities, K_R , on the square root of the geometric mean radius, $(\bar{R})^{1/2}$. \square , 123-bp ladder; \circ , 12B multimer ladder; Δ , 12A multimer ladder.

3.6 Ferguson plots based on relative mobilities

Because of the difficulties encountered in the analysis of the absolute mobilities of the various DNA fragments with the extended Ogston theory, Ferguson plots were also constructed using relative mobilities, as shown in Fig. 9. The slopes of the lines are much less steep than observed with the absolute mobilities (Fig. 4) because of the dependence of the reference mobility on gel concentration (see Section 2.2.4). The slopes of the lines and the intercepts at zero gel concentration were determined by linear regression.

3.7 Gel pore size calculated from relative mobilities

The median pore radius of the various polyacrylamide gels was calculated from the Ferguson plots based on relative mobilities, using both \bar{R} and R_G to estimate DNA size. Log log plots of the estimated pore radius as a function of gel con-

centration are shown in Fig. 10 for each of the three molecular weight ladders. In each case the data were approximated by straight lines determined by linear regression. If \bar{R} was used to estimate DNA macromolecular size, the slopes of the lines ranged from -0.28 to -0.31 for the three molecular weight ladders (Fig. 10a). When DNA size was estimated by R_G , the slopes of the straight lines were -0.54 for the 123-bp ladder, -0.60 for the 12A multimer ladder, and -0.62 for the 12B multimer ladder (Fig. 10b). All of these slopes are close to the value of -0.5 predicted by the extended Ogston theory [30-34]. Hence, R_G is the appropriate measure of DNA size to use for calculating gel pore radii from relative mobility plots. Similar conclusions were drawn from an analysis of the absolute and relative mobilities of DNA fragments in agarose gels [40].

The equations describing the straight lines in Fig. 10b are

$$123\text{-bp ladder: } r_p = 242 T^{-0.54} \quad (8a)$$

$$12B \text{ ladder: } r_p = 340 T^{-0.62} \quad (8b)$$

$$12A \text{ ladder: } r_p = 255 T^{-0.60} \quad (8c)$$

Numerical values of the pore radius as a function of gel concentration, calculated from Eqs. (8), are given in Table 1. Averages of the three values at each gel concentration are also given. Fig. 10b and Table 1 indicate that polyacrylamide gels

ranging from 3.5 to 10.5 % in concentration have effective pore radii ranging from ~130 to ~70 nm, the exact value at each gel concentration depending on the molecular weight ladder used to determine the pore size.

Table 1 Pore radius of gels containing 3 % Bis

%T	123-bp ladder	12B Multimer ladder	12A Multimer ladder	Average
3.5	123 nm	156 nm	120 nm	133 nm
4.6	106	132	102	113
5.7	95	115	90	100
6.9	85	102	80	89
8.1	78	93	73	81
9.3	73	85	67	75
10.5	68	79	62	70

The polyacrylamide gel pore sizes determined using relative mobilities and R_G (Fig. 10b and Table 1) are an order of magnitude larger than the values determined using absolute mobilities and \bar{R} (compare Fig. 6), primarily because of the use of R_G to measure macromolecular size (see [40, 50] and Section 2.2.7 for discussions of this point). Therefore, these pore radii are also an order of magnitude larger than other values in the literature [8, 28-30], all of which were determined using the geometric mean radius [8, 29, 30] or the Stokes radius [28] to estimate macromolecular size. However, the larger effective pore sizes determined using the relative mobilities and R_G are consistent with scanning electron microscope

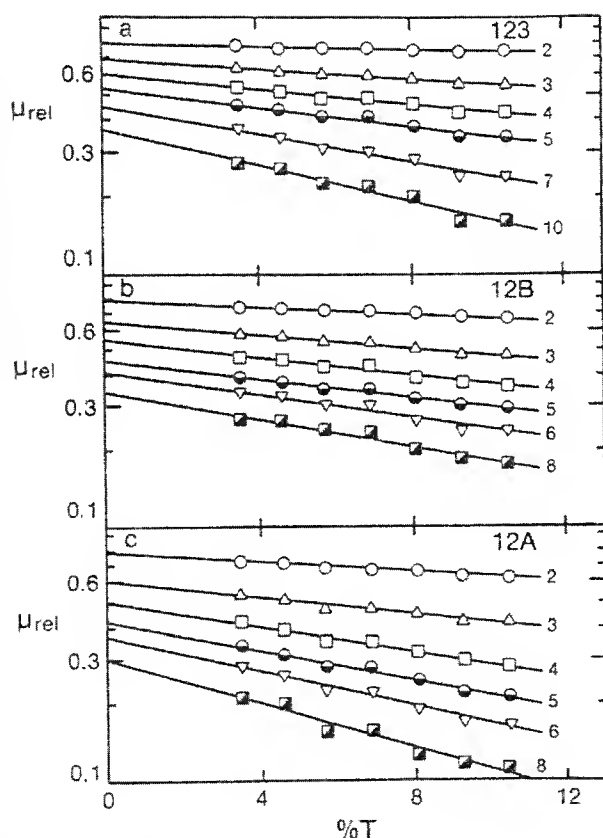


Figure 9. Ferguson plots based on relative mobilities. The logarithm of the relative mobility, μ_{rel} , is plotted as a function of polyacrylamide concentration, %T. (a) 123-bp ladder; (b) 12B multimer ladder; (c) 12A multimer ladder. For each multimer ladder, the number of monomers in each multimer is indicated beside each curve.

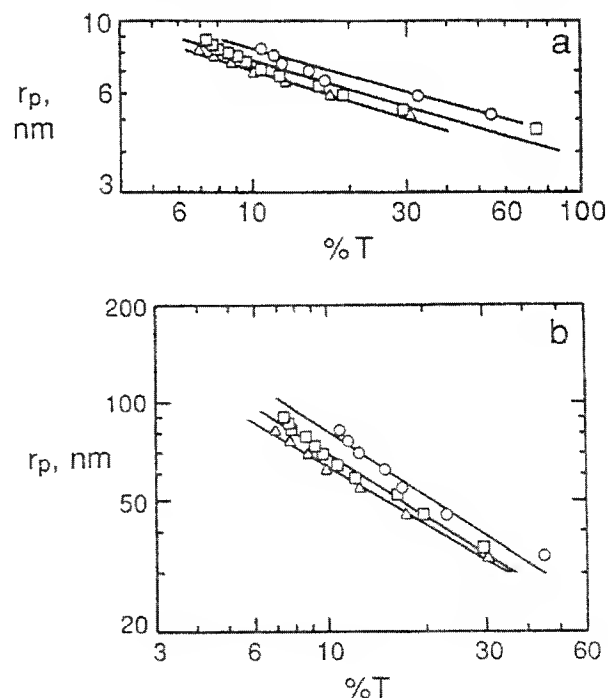


Figure 10. Log-log plots of the effective median gel pore radius, r_p , as a function of gel concentration, %T. The values of %T were calculated from Ferguson plots based on relative mobilities. In (a), DNA molecular size was estimated from \bar{R} ; in (b), DNA size was estimated from R_G . The slopes of the drawn lines, calculated by linear regression, ranged from -0.28 to -0.31 in (a); in (b), the slopes ranged from -0.54 to -0.62. \square , 123-bp ladder; \circ , 12B multimer ladder; Δ , 12A multimer ladder.

studies, which showed that the polyacrylamide matrix has a closed cell structure with relatively thick walls, similar to that of a sponge [72]. The larger pore radii determined here are also consistent with a high resolution transmission electron microscope study of freeze-fractured polyacrylamide gels, which showed that the gels contain pores in the submicron range [73]. More precise estimates of pore size cannot be made because the scale markings were omitted from the micrographs in [73]; however, comparison with [72] suggests that the pore diameters range from 10 to 100 nm, depending on gel composition. These values are of the same order of magnitude as the pore sizes determined in the present study.

Recently, Ceglarek and Revzin [74] and Tietz [34] also questioned the accuracy of the pore sizes traditionally assumed for polyacrylamide gels. It is known that spherical virus particles with diameters of 25 and 30 nm can enter dilute polyacrylamide gels [75] and be resolved [73], suggesting that the pores must be large enough to accommodate particles of this size. In addition, RNA polymerase complexes with DNA restriction fragments freely enter 4% polyacrylamide gels [74], even when the polymerase, with a radius of gyration of 6 nm [76], is bound to the end of the DNA fragment [74]. These results, together with the results reported here, suggest that the pore size of the polyacrylamide matrix must be much larger than previously assumed.

Tietz [34] has also raised the question of whether the extended Ogston theory can be applied to electrophoresis in polyacrylamide gels, if the structure of the gel resembles a sponge rather than a haystack: the Ogston model assumes the existence of a randomly oriented fiber network. However, the Ogston theory was applied successfully to agarose gels [40,

77], even though the structure of agarose appears sponge-like [78] and contains microvoids [79].

3.8 Estimation of gel pore size from Ferguson plots of oligomers of bovine serum albumin

Exactly the same procedure can be used to estimate the pore size of the polyacrylamide matrix from the mobility of bovine serum albumin (BSA) oligomers reported by Hedrick and Smith [80]. The gel concentration at which the mobility of each oligomer is equal to one-half its mobility at zero gel concentration can be estimated from Fig. 3 of [80]. Hydrodynamic studies of BSA indicate that it can be described as a prolate ellipsoid of revolution with a length of 13.8 nm and a diameter of 3.0 nm [81, 82]. X-ray studies of human serum albumin, a molecule very similar to BSA, have shown that it has dimensions of $14.5 \times 5.0 \times 2.2$ nm [83]. If the BSA monomer is assumed to have a hydrated length of 15 nm, and the dimer and trimer are assumed to be end-to-end aggregates with lengths $2 \times$ and $3 \times$ the length of the monomer, the mobilities of the various oligomers can be used to estimate the median pore size of the polyacrylamide matrix. A log-log plot of the estimated pore radius as a function of %T is given in Fig. 11. The estimated pore radius is found to decrease from 100 to 17 nm over the gel concentration range of 3.5–10.5 %T. If the BSA oligomers are not aligned end-to-end, but overlap each other by $\sim 50\%$ ([82], also Oncley, J. L., personal communication cited in [83]) the dotted line in Fig. 11 is obtained. Using this correlation, the estimated pore radius decreases from 36–12 nm when the gel concentration increases from 3.5 to 10.5 %T. The corresponding values of the pore radii estimated from the mobility of DNA oligomers (Fig. 10b) range from 130 to 70 nm over the same gel concentration range. Hence the pore sizes determined from the mobility of BSA oligomers are of the same order of magnitude as those determined using DNA restriction fragments, as long as the external dimensions of the BSA molecule are used as the measure of macromolecular size. The pore sizes estimated from the BSA oligomers are more uncertain than the pore sizes estimated from the DNA fragments, because the end-to-end lengths of the BSA oligomers are not well characterized.

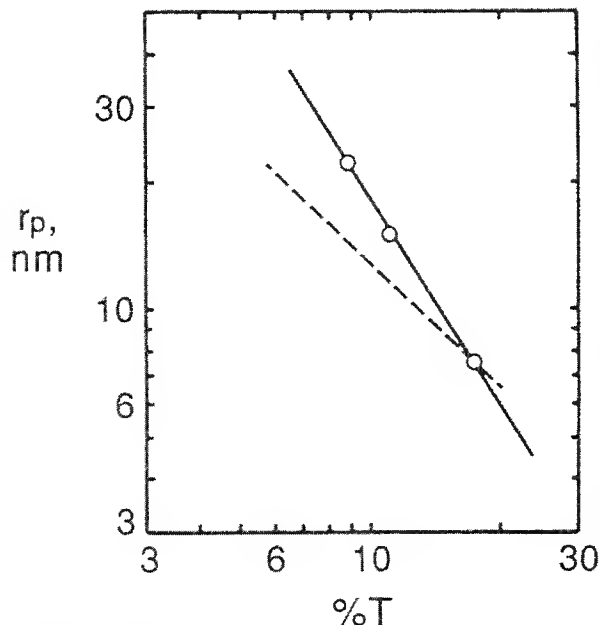


Figure 11. Log-log plot of the dependence of the estimated gel pore radius, r_p , of BSA oligomers on gel concentration, %T. The mobilities were taken from [80]. ○ The half-lengths of the oligomers were based on the assumption that the dimer and trimer were $2 \times$ and $3 \times$ the length of the monomer. The dotted line is drawn on the assumption that the dimer and trimer were $1.5 \times$ and $2 \times$ the length of the monomer, respectively.

3.9 Gel fiber parameters calculated from retardation coefficients based on relative mobilities

In order to estimate the gel fiber parameters, the square roots of the retardation coefficients calculated from the Ferguson plots based on relative mobilities (Fig. 9) were plotted as a function of R_G , as shown in Fig. 12. If the curvature at the lowest molecular weights is ignored, the data can be approximated by straight lines, which extrapolate to negative intercepts of 13–18 nm (average = 15 ± 2 nm) at $(K_R)^{1/2} = 0$. According to the extended Ogston theory, this negative intercept is equal to the effective gel fiber radius [30, 32, 34]. Since all three data sets extrapolated to approximately the same value, the effective gel fiber radius appears to be independent of DNA sequence. The apparent fiber radius determined in Fig. 12 is much larger than the previously estimated value of ~ 1 nm [8, 29, 30, 32, 84], primarily because of the use of R_G to estimate DNA size. Previous studies were scaled by using the geometric mean radius or the Stokes radius to estimate macromolecular size. A larger fiber radius of 10 nm was reported for the polyacrylamide matrix from the electrophoresis of RNA molecules [85].

The slopes of the lines in Fig. 12 were used to estimate the total gel fiber length, as described in Section 2.2.6. The fiber length, P , was found to be 2.1×10^{10} cm/g acrylamide for the 12B multimer ladder, 3.1×10^{10} cm/g for the 123-bp ladder, and 3.6×10^{10} cm/g for the 12A multimer ladder. These values are 1–2 orders of magnitude smaller than previously determined values, again because of the use of R_G instead of \bar{R} to determine macromolecular size. However, the significance of these values is dependent on the validity of the extended Ogston theory to describe electrophoresis in polyacrylamide gels (see also [34]).

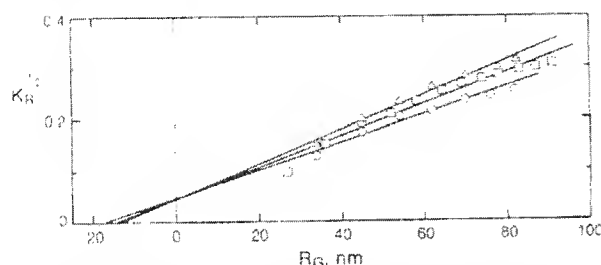


Figure 12. Dependence of the square root of the retardation coefficient, $(K_R)^{1/2}$, on R_G . The retardation coefficients were calculated from the relative mobilities in Fig. 9. \square , 123-bp ladder; \circ , 12B multimer ladder; Δ , 12A multimer ladder.

3.10 Dependence of retardation coefficients on molecular radius

To see if $K_R^{-1/2}$ vs. R_G is the best method of plotting the electrophoresis data, the retardation coefficients determined from Ferguson plots based on relative mobilities were also plotted as K_R vs. R_G , as shown in Fig. 13. The retardation coefficients of all three molecular weight ladders can be described by straight lines, all of which extrapolate to $K_R = 0$ at $R_G \sim 19$ nm. The extrapolation of K_R to zero at finite R_G is due to the fact that the K_R values were determined from relative mobilities, using the mobility of the smallest molecule in each data set as the reference mobility. The relative mobility of the reference fragment is defined to be 1.00 at all gel concentrations. Therefore, the Ferguson plot of the reference fragment is a horizontal line, the slope of which (equal by definition to $-K_R$) is zero. The value of R_G at which $K_R = 0$ is ~ 19 nm, close to the R_G of the reference fragments ($R_G = 19.5$ nm for the 12A and

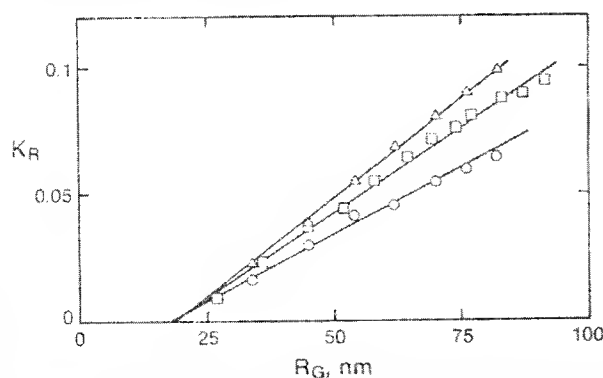


Figure 13. Dependence of the retardation coefficients, K_R , calculated from the relative mobilities in Fig. 9, on R_G . \square , 123-bp ladder; \circ , 12B multimer ladder; Δ , 12A multimer ladder.

12B monomers, and 15 nm for the 123-bp fragment). Further discussion of the relationship between the retardation coefficients and molecular radius will be deferred to part IV of this series. Plots of K_R vs. \bar{R} were also linear, and extrapolated to $K_R = 0$ at $\bar{R} = 4.3 \pm 0.1$ nm (not shown). This value of \bar{R} is close to the value of \bar{R} calculated for the various monomer fragments ($\bar{R} = 4.1$ nm for fragments 12A and 12B and 3.8 nm for the 123-bp fragment), as expected. These plots are not illustrated because R_G appears to be the appropriate measure of DNA size to use in conjunction with Ferguson plots based on relative mobilities.

4 Concluding remarks

In this study the pore sizes of polyacrylamide gels containing 3% Bis were estimated from the mobilities of a variety of DNA restriction fragments by constructing Ferguson plots for each fragment and determining the gel concentration at which the mobility was equal to one half the mobility at zero gel concentration [40, 45, 50]. At this gel concentration, the median pore radius of the gel should be equal to the radius of the migrating macromolecule [29, 32, 33, 44–46]. This method of determining gel pore size depends only on the assumption that half the available spaces in the gel are accessible to a migrating macromolecule at $\mu = \mu_0/2$. Two types of Ferguson plots were compared, based on absolute mobilities and relative mobilities. Two measures of DNA macromolecular size were also considered: the geometric mean radius and the rms radius of gyration. When the pore sizes were calculated from Ferguson plots based on absolute mobilities and the geometric mean radius was used to measure DNA size, the calculated gel pore sizes were in agreement with previously determined values [8, 28–30]. However, the Ogston equations were not obeyed and it was not possible to determine gel fiber parameters by this method. The results were not improved by using R_G instead of \bar{R} to measure DNA size. When the mobility data were analyzed using relative mobilities in conjunction with the rms radius of gyration, the gel pore radii were about an order of magnitude larger than previously determined values, because of the use of R_G instead of \bar{R} to measure DNA size. However, these larger pore radii are in agreement with transmission electron microscope studies of freeze fractured polyacrylamide gels [73, 74]. In addition, using this method of analysis the Ogston equations are obeyed and the gel fiber parameters can be estimated. Gel pore sizes of the same order of magnitude can be estimated from the mobility of BSA oligomers [80] in polyacrylamide gels. Hence, the major conclusion of this paper is that 3.5–10.5% polyacrylamide gels crosslinked with 3% Bis contain pores ranging from 130 to 70 nm in effective radius.

The gel pore radii determined in the present study are median pore radii. The pore radii determined in the conventional manner from the extended Ogston theory are mean pore radii [29, 30, 32–34], which would probably be about 10% larger [29] than the values reported here. The similarity of the gel pore radii calculated from the mobility of BSA and DNA oligomers suggests that the effective pore size of the polyacrylamide matrix is independent of the type of probe used for the measurements, as long as the external dimensions of the probe are used to estimate the size of the macromolecule. Similar results were observed with agarose gels [40]. However, more studies of the pore size of the polyacrylamide matrix are needed, especially studies with probes of known size. More

definitive solid state measurements are also needed for comparison with the dynamic measurements.

Financial support of this work by Grant No. 29690 from the National Institute of General Medical Sciences is gratefully acknowledged.

Received September 12, 1990

5 References

- Trifonov, E. N., *CRC Crit. Rev. Biochem.* 1985, **19**, 89-106.
- Stellwagen, N. C., *Adv. Electrophoresis* 1987, **1**, 179-228.
- Dickmann, S., in: Fekstein, F. and Lilley, D. (Eds.), *Nucleic Acids and Molecular Biology*, Springer, Berlin 1987, pp. 138-156.
- Sundaralingam, M. and Sekharudu, Y. C., in: Olson, W. K., Sarma, M. H., Sarma, R. H. and Sundaralingam, M. (Eds.), *Structure and Expression, Vol. 3: DNA Bending and Curvature*, Adenine Press, Schenectady, New York 1988, pp. 9-37.
- Mertz, J. E. and Berg, P., *Proc. Natl. Acad. Sci. USA* 1974, **71**, 4879-4883.
- Marmitt, T., Jeffrey, A., and van de Sande, H., *Biochemistry* 1975, **14**, 3787-3794.
- Marini, J. D., Levene, S. D., Crothers, D. M., and Englund, P. T., *Proc. Natl. Acad. Sci. USA* 1982, **79**, 7664-7668.
- Stellwagen, N. C., *Biochemistry* 1983, **22**, 6186-6193.
- Anderson, J. N., *Nucleic Acids Res.* 1986, **14**, 8513-8533.
- Dickmann, S. and Wang, J. C., *J. Mol. Biol.* 1985, **186**, 1-11.
- Hagerman, P. J., *Biochemistry* 1985, **24**, 7033-7037.
- Koepsel, R. R. and Khan, S. A., *Science* 1986, **233**, 1316-1318.
- Bossa, L. and Smith, D. M., *Cell* 1984, **39**, 643-652.
- Griffith, J., Bleyman, M., Rauch, C. A., Kitchin, P. A., and Englund, P. T., *Cell* 1986, **46**, 717-724.
- Thervey, B., Coulaud, B., LeBret, M., and Revet, B., in: Olson, W. K., Sarma, M. H., Sarma, R. H., and Sundaralingam, M. (Eds.), *Structure and Expression, Vol. 3: DNA Bending and Curvature*, Adenine Press, Schenectady, 1988, pp. 39-55.
- Ulanovsky, V., Bodner, M., Trifonov, E. N., and Choder, M., *Proc. Natl. Acad. Sci. USA* 1986, **83**, 862-866.
- Zahn, K. and Blattner, F. R., *Science* 1987, **236**, 416-422.
- Stellwagen, N. C., *Biophys. Chem.* 1982, **15**, 311-316.
- Hagerman, P. J., *Proc. Natl. Acad. Sci. USA* 1984, **81**, 4632-4636.
- Levene, S. D., Wu, H.-M., and Crothers, D. M., *Biochemistry* 1986, **25**, 3988-3995.
- Stellwagen, N. C. and Stellwagen, A., in: Schafer Nielsen, C. (Ed.), *Electrophoresis '88*, VCH Publishers, Weinheim 1988, pp. 383-399.
- Marini, J. D., Trifon, P. N., Goodman, T. C., Singleton, C. K., Wells, R. D., Wartell, R. M., and Englund, P. T., *J. Biol. Chem.* 1984, **259**, 8954-8979.
- Stellwagen, A. and Stellwagen, N. C., *Biopolymers* 1990, **30**, 309-324.
- Wu, H.-M. and Crothers, D. M., *Nature* 1984, **308**, 509-513.
- Calladine, C. R., Drew, H. R., and McCall, M. J., *J. Mol. Biol.* 1985, **201**, 127-137.
- Koo, H. S. and Crothers, D. M., *Proc. Natl. Acad. Sci. USA* 1988, **85**, 1767-1767.
- Cacchione, S., DeSantis, P., Foti, D., Palleschi, A., and Savino, M., *Biochemistry* 1989, **28**, 8706-8713.
- Forbbs, M. P., *Anal. Biochem.* 1965, **13**, 121-132.
- Fawcett, J. S. and Morris, C. J. O. R., *Sep. Science* 1966, **1**, 9-26.
- Chrambach, A. and Rodbard, D., *Science* 1971, **170**, 440-451.
- Opston, A. G., *Trans. Faraday Soc.* 1958, **54**, 1754-1757.
- Rodbard, D. and Chrambach, A., *Proc. Natl. Acad. Sci. USA* 1970, **65**, 907-917.
- Rodbard, D., in: Csiszaropoulos, N. (Ed.), *Methods of Protein Separation*, Vol. 2, Plenum, New York 1976, pp. 145-179.
- Tietz, D., *Adv. Electrophoresis* 1988, **2**, 159-169.
- Perreguer, K. A., *Metabolism* 1964, **13**, 985-1002.
- Sutcliffe, J. G., *Cold Spring Harbor Symp. Quant. Biol.* 1978, **42**, 77-90.
- Stellwagen, N. C., *Biochemistry* 1984, **23**, 6311-6319.
- Marmitt, T., Fréchet, F. F., and Sambrook, J., *Molecular Cloning, A Laboratory Manual*, Cold Spring Harbor Laboratory, Cold Spring Harbor, N. Y. 1982, p. 175.
- Bishop, D. H. L., Claybrook, J. R. and Spiegelman, S., *J. Mol. Biol.* 1967, **26**, 373-387.
- Holmes, D. L. and Stellwagen, N. C., *Electrophoresis* 1990, **11**, 649-652.
- Orbán, L., Fawcett, J. S., Tietz, D. and Chrambach, A., *Electrophoresis* 1989, **10**, 254-259.
- Richards, E. G., Coll, J. A. and Grätzer, W. B., *Anal. Biochem.* 1965, **12**, 452-471.
- Butterman, M., Tietz, D., Orbán, L., and Chrambach, A., *Electrophoresis* 1988, **9**, 293-298.
- Laurent, T. C. and Killander, J., *J. Chromatogr.* 1964, **14**, 317-350.
- Stellwagen, N. C., *Biopolymers* 1985, **24**, 2243-2255.
- Slater, G. W., Noolandi, J., Tarnai, C. and Lalonde, M., *Biopolymers* 1988, **27**, 509-524.
- Giddings, J. C., Kucera, E., Russel, C. P. and Myers, M. N., *J. Phys. Chem.* 1968, **72**, 4397-4408.
- Ogston, A. G., Preston, B. N. and Wells, J. D., *Proc. Roy. Soc. London* 1973, **A333**, 297-316.
- Cobbs, G., *Biophys. J.* 1981, **35**, 535-542.
- Holmes, D. L. and Stellwagen, N. C., *Electrophoresis* 1990, **11**, 5-15.
- Benoit, H. and Doty, P., *J. Phys. Chem.* 1953, **57**, 958-963.
- Hagerman, P. J., *Annu. Rev. Biophys. Biophys. Chem.* 1988, **17**, 265-286.
- Borochof, N., Eisenberg, H. and Kam, Z., *Biopolymers* 1981, **20**, 231-235.
- Kam, A., Borochof, N. and Eisenberg, H., *Biopolymers* 1981, **20**, 2671-2690.
- Krarky, G. and Porod, G., *Rec. Trav. Chim.* 1949, **68**, 1106-1113.
- Eisenberg, H., *Accounts Chem. Res.* 1987, **20**, 276-282.
- Cairney, K. L. and Harrington, R. E., *Biopolymers* 1982, **21**, 923-934.
- Hagerman, P., *Biopolymers* 1981, **20**, 1503-1525.
- Flas, J. G. and Eden, D., *Macromolecules* 1981, **14**, 410-419.
- Frontali, C., Dore, E., Ferranto, A., Gratton, E., Battini, A., Pozzan, M. R. and Valdevit, E., *Biopolymers* 1979, **18**, 1353-1373.
- Taylor, W. H. and Hagerman, P. J., *J. Mol. Biol.* 1990, **212**, 363-376.
- Lerman, L. S. and Frisch, H. L., *Biopolymers* 1982, **21**, 995-997.
- Lumpkin, O. J. and Zimm, B. H., *Biopolymers* 1982, **21**, 2315-2316.
- Lumpkin, O. J., DeJardin, P. and Zimm, B. H., *Biopolymers* 1985, **24**, 1573-1593.
- Slater, G. W. and Noolandi, J., *Biopolymers* 1986, **24**, 1513-1593.
- Fisher, M. P. and Dingman, C. W., *Biochemistry* 1971, **10**, 1895-1899.
- Olivera, B. M., Ruine, P. and Davidson, N., *Biopolymers* 1964, **2**, 245-257.
- Ross, P. D. and Scruggs, R. L., *Biopolymers* 1964, **2**, 79-89.
- Ross, P. D. and Scruggs, R. L., *Biopolymers* 1964, **2**, 231-236.
- Serwer, P. and Allen, J. L., *Biochemistry* 1984, **23**, 922-927.
- Serwer, P. and Hayes, S. J., *Electrophoresis* 1982, **3**, 80-85.
- Rüchel, R. and Bräger, M. D., *Anal. Biochem.* 1975, **68**, 415-428.
- Rüchel, R., Steere, R. L. and Erbe, F. F., *J. Chromatogr.* 1978, **166**, 563-575.
- Ceglarek, J. A. and Revzin, A., *Electrophoresis* 1989, **10**, 360-365.
- Hutchison, C. A., Edgell, M. H. and Sinsheimer, R. L., *J. Mol. Biol.* 1967, **23**, 553-575.
- Pilz, I., Kratky, O. and Rabassay, D., *Eur. J. Biochem.* 1972, **28**, 205-220.
- Serwer, P. and Hayes, S. J., *Anal. Biochem.* 1986, **158**, 72-78.
- Amsterdam, A., Er-El, Z. and Shaltiel, S., *Arch. Biochem. Biophys.* 1975, **171**, 673-677.
- Attwood, T. K., Nelmes, B. J. and Sellen, D. R., *Biopolymers* 1988, **27**, 201-212.
- Hedrick, J. L. and Smith, A. J., *Arch. Biochem. Biophys.* 1968, **126**, 155-164.
- Moser, P., Squire, P. G. and O'Konski, C. T., *J. Phys. Chem.* 1966, **70**, 744-746.
- Squire, P. G., Moser, P. and O'Konski, C. T., *Biochemistry* 1968, **7**, 4261-4272.
- Low, B. W., *J. Am. Chem. Soc.* 1952, **74**, 4830-4834.
- Rodbard, D. and Chrambach, A., *Anal. Biochem.* 1971, **40**, 95-134.
- Richards, F. G. and Lecanidou, R., *Anal. Biochem.* 1971, **40**, 43-71.